

2

FTD-ID(RS)T-1001-84

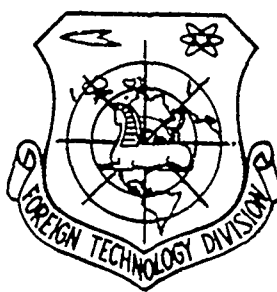
# FOREIGN TECHNOLOGY DIVISION



PROBLEMS ON THE DIFFRACTION AND PROPAGATION OF WAVES  
(Selected Articles)

AD-A145 139

DTIC FILE COPY



DTIC  
ELECTE  
SEP 04 1984  
S E D

Approved for public release;  
distribution unlimited.

84 08 30 072

## UNEDITED MACHINE TRANSLATION

FTD-ID(RS)T-1001-84

9 August 1984

MICROFICHE NR: FTD-84-C-000796

PROBLEMS ON THE DIFFRACTION AND PROPAGATION OF WAVES  
(Selected Articles)

English pages: 118

Source: Problemy Difraktsii i Rasprostraneniya Voln,  
Nr. 11, Leningrad, 1972, pp. 3-32; 33-56;  
201-204

Country of origin: USSR

This document is a machine translation

Requester: FTD/TQFE

Approved for public release; distribution unlimited.

THIS TRANSLATION IS A RENDITION OF THE ORIGINAL FOREIGN TEXT WITHOUT ANY ANALYTICAL OR EDITORIAL COMMENT. STATEMENTS OR THEORIES ADVOCATED OR IMPLIED ARE THOSE OF THE SOURCE AND DO NOT NECESSARILY REFLECT THE POSITION OR OPINION OF THE FOREIGN TECHNOLOGY DIVISION.

PREPARED BY:

TRANSLATION DIVISION  
FOREIGN TECHNOLOGY DIVISION  
WP-AFB, OHIO.

# TABLE OF CONTENTS

U. S. Board on Geographic Names Transliteration System.....	ii
Eigenvalues of Normal Waves in a Plane Waveguide Channel, by G. I. Makarov, V. V. Novikov.....	1
Electromagnetic Field in a Plane Thin Waveguide, by G. I. Makarov, V. V. Novikov.....	60
Supplement and Revision to the Article "On the Tropospheric Refraction of Radio Waves", by G. I. Makarov, N. P. Tikhomirov.....	112

Accession for	
NTIS GRA&I	<input checked="" type="checkbox"/>
DTIC TAB	<input type="checkbox"/>
Unannounced	<input type="checkbox"/>
Justification	
By	
Distribution/	
Availability Codes	
Dist	Avail and/or Special
A-1	



# U. S. BOARD ON GEOGRAPHIC NAMES transliteration SYSTEM

Block	Italic	Transliteration	Block	Italic	Transliteration
А а	<i>А а</i>	A, a	Р р	<i>Р р</i>	R, r
Б б	<i>Б б</i>	B, b	С с	<i>С с</i>	S, s
В в	<i>В в</i>	V, v	Т т	<i>Т т</i>	T, t
Г г	<i>Г г</i>	G, g	У у	<i>У у</i>	U, u
Д д	<i>Д д</i>	D, d	Ф ф	<i>Ф ф</i>	F, f
Е е	<i>Е е</i>	Ye, ye; E, e*	Х х	<i>Х х</i>	Kh, kh
Ж ж	<i>Ж ж</i>	Zh, zh	Ц ц	<i>Ц ц</i>	Ts, ts
З з	<i>З з</i>	Z, z	Ч ч	<i>Ч ч</i>	Ch, ch
И и	<i>И и</i>	I, i	Ш ш	<i>Ш ш</i>	Sh, sh
Й й	<i>Й й</i>	Y, y	Щ щ	<i>Щ щ</i>	Shch, shch
К к	<i>К к</i>	K, k	Ъ ъ	<i>Ъ ъ</i>	"
Л л	<i>Л л</i>	L, l	Ы ы	<i>Ы ы</i>	Y, y
М м	<i>М м</i>	M, m	Ь ь	<i>Ь ь</i>	'
Н н	<i>Н н</i>	N, n	Э э	<i>Э э</i>	E, e
О о	<i>О о</i>	O, o	Ю ю	<i>Ю ю</i>	Yu, yu
П п	<i>П п</i>	P, p	Я я	<i>Я я</i>	Ya, ya

\*ye initially, after vowels, and after ъ, ь; e elsewhere.  
When written as ё in Russian, transliterate as yě or ě.

## RUSSIAN AND ENGLISH TRIGONOMETRIC FUNCTIONS

Russian	English	Russian	English	Russian	English
sin	sin	sh	sinh	arc sh	sinn <sup>-1</sup>
cos	cos	ch	cosh	arc ch	cosn <sup>-1</sup>
tg	tan	th	tanh	arc th	tann <sup>-1</sup>
ctg	cot	cth	coth	arc cth	coth <sup>-1</sup>
sec	sec	sch	sech	arc sch	sech <sup>-1</sup>
cosec	csc	csch	csch	arc csch	csch <sup>-1</sup>

Russian English

rot curl  
lg log

## GRAPHICS DISCLAIMER

All figures, graphics, tables, equations, etc.  
merged into this translation were extracted  
from the best quality copy available.

Page 3.

# EIGENVALUES OF NORMAL WAVES IN A PLANE WAVEGUIDE CHANNEL.

G. I. Makarov, V. V. Novikov.

In preceding works [1-2] the qualitative investigation of the behavior of the eigenvalues of the transverse operator of the problem of the propagation of electromagnetic waves in the flat/plane and spherical waveguide channels was carried out. In this case it was assumed that the lower (internal) wall of waveguide is ideally conducting, and on the upper wall impedance type approximate boundary conditions were used. It is of interest to explain, to what changes in the behavior of eigenvalues the use of strict boundary conditions on the upper waveguide will bring. In the present work this question for the flat/plane waveguide will be examined. Since while conducting of qualitative investigations it is necessary to have sufficiently simple analytical expression for the surface impedance (or reflection coefficient) of upper wall water/aqueous-water, appropriate by strip wave with the assigned, generally speaking, complex angle of

incidence, we will be bounded to the examination of the problem of the propagation of electromagnetic waves in the three-layered medium and for simplicity we will count as in the preceding/previous works, that the lower semi-infinite layer is ideally conducting. Analogous problem was examined in the series/row of works [3-6], in which was conducted the investigation of the behavior of the eigenvalues of normal waves in some particular situations. The purpose of this work is a more complete analysis of the characteristic equation for eigenvalues and the isolation/liberation of the continuous part of the spectrum.

#### § 1. Representation of the solution of problem in the form of the sum of normal waves.

In the present paragraph we will briefly reproduce the construction of the solution of the problem about the field of vertical electric dipole in the plane-layered medium, which consists of three uniform layers, two of which are semi-infinite, and let us lead the necessary for further investigation transformations of solution.

Page 4.

In the cylindrical coordinate system  $(r, \varphi, z)$  the surfaces of

layers are described by equations  $z=0$  and  $z=h$ , and dipole is located at point  $r=0$ ,  $z=z_0$ . (Fig. 1). Lower medium possesses infinite conductivity ( $\sigma_0=\infty$ ), upper medium is isotropic, uniform and possesses relative dielectric constant  $\epsilon_m$  and conductivity  $\sigma_m$ , and layer arranged/located between them, is vacuum. As it will interest the solution of stationary problem with the dependence of current in the dipole on the time of form  $e^{-i\omega t}$ . Mathematical problem is reduced to the construction of the solution of the equations of Maxwell, who satisfies the appropriate boundary conditions, including at infinity (with  $z\rightarrow\infty$ ). For obtaining the solution of problem in the form of the series/row of normal waves it would be possible to immediately seek it in the form of eigenfunction expansion of transverse operator. But since in this case (in contrast to the approximate impedance setting) transverse operator together with the discrete/digital possesses continuous spectrum, that complicates construction the solution in this way, which is expedient to construct solution standardly, utilizing an expansion in the spectral functions of radial operator, i.e., the integral transform of Fourier-Bessel, and then to reduce him to the series/row of normal waves and the integral along the continuous spectrum of transverse operator.

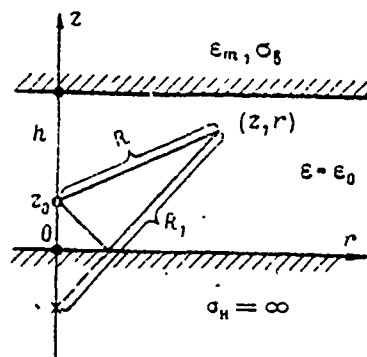


Fig. 1.

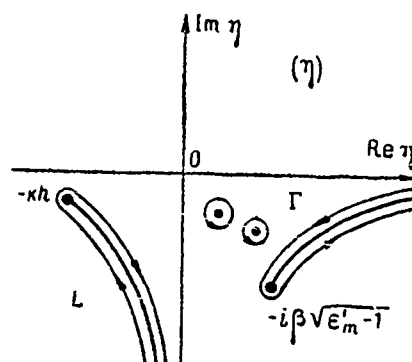


Fig. 2.

Page 5.

Introducing vector potential  $A = Ae_z$  and utilizing transformation of Fourier-Bessel during the solution of the equation of Helmholtz for the potential, it is not difficult to obtain the following integral representation for potential ( $0 \leq z \leq h$ );

$$A = \frac{I h_g}{4\pi} \int_{-\infty}^{+\infty} \frac{H_0^{(1)}(\lambda r)}{\sqrt{k^2 - \lambda^2}} \frac{Q(\lambda)}{\Delta(\lambda)} \lambda d\lambda, \quad (1)$$

where  $I$  - current in the foundation of dipole,  $h_g$  - its effective height,

$$Q(\lambda) = \begin{cases} [i\sqrt{k^2 \epsilon'_m - \lambda^2} \sin \sqrt{k^2 - \lambda^2} (h - z_0) - \\ - \epsilon'_m \sqrt{k^2 - \lambda^2} \cos \sqrt{k^2 - \lambda^2} (h - z_0)] \cos \sqrt{k^2 - \lambda^2} z \text{ при } 0 \leq z \leq z_0, \\ [i\sqrt{k^2 \epsilon'_m - \lambda^2} \sin \sqrt{k^2 - \lambda^2} (h - z) - \\ - \epsilon'_m \sqrt{k^2 - \lambda^2} \cos \sqrt{k^2 - \lambda^2} (h - z)] \cos \sqrt{k^2 - \lambda^2} z_0 \text{ при } z_0 \leq z \leq h, \end{cases}$$

$$\Delta(\lambda) = i\epsilon'_m \sqrt{k^2 - \lambda^2} \sin \sqrt{k^2 - \lambda^2} h - \sqrt{k^2 \epsilon'_m - \lambda^2} \cos \sqrt{k^2 - \lambda^2} h,$$

Key: (1).



$k$  - wave number in the vacuum,  $\varepsilon'_m = \varepsilon_m + i \frac{\sigma_m}{\omega \varepsilon_0}$  - the complex relative dielectric constant of upper medium. In the expressions for  $Q(\lambda)$  and  $\Delta(\lambda)$  the branch of function  $\sqrt{k^2 \varepsilon'_m - \lambda^2}$  is fixed/recorded by the condition

$$\operatorname{Im} \sqrt{k^2 \varepsilon'_m - \lambda^2} > 0. \quad (2)$$

As far as function  $\sqrt{k^2 - \lambda^2}$  is concerned, fixation of its branch is arbitrary, since the integrand of integral (1) does not have a branching at points  $\lambda = k$ . The components of electromagnetic field are expressed as potential  $A$  with the help of the differential relationships/relations (with  $0 \leq r \leq h$ )

$$H_r = -\frac{\partial A}{\partial r}, \quad E_r = -\frac{1}{i\omega \varepsilon_0} \frac{\partial^2 A}{\partial z \partial r}, \quad E_z = \frac{1}{i\omega \varepsilon_0} \frac{1}{r} \frac{\partial}{\partial r} \left( r \frac{\partial A}{\partial r} \right).$$

During the representation of solution (1) in the form of the series/row of normal waves expediently for convenience in the comparison with the results of the problem in the approximate impedance setting of passing in integral (1) to the new variable of the integration

$$\eta = \sqrt{k^2 - \lambda^2} h, \quad \operatorname{Im} \sqrt{k^2 - \lambda^2} h = \operatorname{Im} \eta \leq 0,$$

as a result of what (1) accepts the form

$$A = -\frac{i h g}{4 \pi h} \int_L H_0^{(1)} \left( \sqrt{k^2 - \frac{\eta^2}{h^2}} r \right) \frac{\tilde{Q}(\eta)}{\tilde{\Delta}(\eta)} d\eta, \quad (3)$$

where

$$\begin{aligned} \widetilde{Q}(\eta) &= \\ &= \begin{cases} \left[ i\eta^* \sin \eta \left( 1 - \frac{z_0}{h} \right) - \varepsilon'_m \eta \cos \eta \left( 1 - \frac{z_0}{h} \right) \right] \cos \eta \frac{z}{h}, & 0 \leq z \leq z_0, \\ \left[ i\eta^* \sin \eta \left( 1 - \frac{z}{h} \right) - \varepsilon'_m \eta \cos \eta \left( 1 - \frac{z}{h} \right) \right] \cos \eta \frac{z_0}{h}, & z_0 \leq z \leq h, \end{cases} \\ \widetilde{\Delta}(\eta) &= i\varepsilon'_m \eta \sin \eta - \eta^* \cos \eta, \quad \eta^* = \sqrt{\eta^2 + \beta^2 (\varepsilon'_m - 1)}, \quad \beta = kh, \end{aligned}$$

in this case  $\operatorname{Im} \eta^* \geq 0$  in view of condition (2), and the branch of function  $\sqrt{k^2 - \frac{\eta^2}{h^2}}$  is fixed/recorded by condition  $\operatorname{Im} \sqrt{k^2 - \frac{\eta^2}{h^2}} \geq 0$ .

Page 6.

The contour of integration L goes along the coasts of section/cut

$\text{Im} \sqrt{k^2 - \frac{\eta^4}{h^2}} = 0$  and in Fig. 2, where it is given for the case, is shown, when wave number  $k$  possesses a small imaginary part ( $\text{Im } k > 0$ ).

The integrand of integral (3) in the lower half-plane of complex plane ( $\eta$ ), besides branch point  $\eta = -kh$ , has pole, caused by bullets  $\tilde{\Delta}(\gamma)$ , and it possesses one additional branch point  $\eta = -i\beta \sqrt{\varepsilon_m' - 1}$  of function  $\eta^*$ , for uniformization of which the section/cut along line  $\text{Im } \eta^* = 0$  is carried out and branch  $\text{Im } \eta^* \geq 0$  is selected.

The duct/contour of integration  $L$  in integral (3) with the real axis is consistent. In this case they will be isolated deductions in poles, which lie at the lower half-plane on the upper sheet of Riemann surface for the function  $\eta^*$ , which is fixed/recorded by condition  $\text{Im } \eta^* \geq 0$ , and will arise integral on the duct/contour  $G$

(Fig. 2), which encompasses section/cut  $\text{Im } \eta^* = 0$ . Integral along the real axis is equal to zero in view of the odd parity of integrand in integral (3), so that as a result we come to the following representation of solution:

$$A = \frac{ihg}{2\pi h} \left\{ \pi \sum_n f_n(z) f_n(z_0) \Lambda_n H_0^{(1)} \left( kr \sqrt{1 - \frac{\eta_n^2}{\beta^2}} \right) - \right. \\ \left. - \frac{1}{2} \int_{\gamma^*} H_0^{(1)} \left( \sqrt{k^2 - \frac{\eta^2}{h^2}} r \right) \frac{\bar{Q}(\eta)}{\Delta(\eta)} d\eta \right\}, \quad (4)$$

in which  $f_n(z) = \cos \eta_n \frac{z}{h}$ ,  $f_n(z_0) = \cos \eta_n \frac{z_0}{h}$  — the so-called transverse functions or high-altitude factors,  $\Lambda_n$  — excitation coefficients

$$\Lambda_n = \frac{1}{1 + \frac{\sin 2\eta_n}{2\eta_n} + \frac{\cos^2 \eta_n}{\epsilon_m \eta_n \sin \eta_n}} = \frac{1}{1 - \frac{i\beta^2 \epsilon_m}{\eta_n^* [\eta_n^2 (\epsilon_m + 1) - \beta^2]}}, \quad (5)$$

$\eta_n$  we the roots of equation  $\Delta(\eta) = 0$

$$i\epsilon_m \eta \text{tg } \eta = \eta^*, \quad \eta^* = \sqrt{\eta^2 + \beta^2 (\epsilon_m - 1)}, \quad (6)$$

located on the upper sheet of riemann surface for  $\eta^*$

Expression (4) is the decomposition of solution in the series/row by the eigenfunctions of the transverse operator of the problems, which on the interval  $0 \leq z \leq h$  coincide with transverse functions  $f_n(z)$ , and integral in the functions of the continuous spectrum of this operator. Follows the terminology, introduced to P. Ye. Krasnushkin [7] and L. M. Brekhovskikh [4], we will call series/row according to the eigenfunctions the series of normal waves, and integral term in (4) — by side wave.

Equation (6) is characteristic equation for the eigenvalues of the transverse operator of problem,  $\mu$ , connected with  $\eta$  relation [1]

$$\eta = \beta \sqrt{\mu}.$$

In this work we will conduct qualitative research of the behavior of eigenvalues in the dependence on the parameters of waveguide and frequency of electromagnetic vibrations and let us compare results with the results of problem in the approximate impedance setting. In the latter case transverse operator possesses purely discrete spectrum [1] and expression for the potential takes the form

$$A_{np} = -\frac{i h_g}{2h} \sum_{n=0}^{\infty} f_n(z) f_n(z_0) \lambda_n^{(np)} H_0^{(1)} \left( kr \sqrt{1 - \frac{\eta_n^2}{\beta^2}} \right), \quad (7)$$

where  $f_n(z)$  and  $f_n(z_0)$  has the same expression, that also in (4),

$$\lambda_n^{(np)} = \frac{1}{1 + \frac{\sin 2\eta_n}{2\eta_n}} = \frac{1}{1 + \frac{t}{t^2 + \eta_n^2}}, \quad (8)$$

$\eta_n$  are the roots of the equation

$$\eta_1 \operatorname{tg} \eta_1 = t, \quad (9)$$

$$t = -i\delta\beta, \quad \delta = \frac{1}{\sqrt{\epsilon_m^2 + 1}}. \quad (10)$$

Characteristic equation upon a strict setting of problem (6) for the form is reduced to the characteristic equation upon impedance

setting (9), but in this case it is necessary to consider the dependence of the given surface impedance on the eigenvalue, i.e., from the angle of incidence in the normal wave on the wall of waveguide, and to assume/set

$$\delta = \delta(\eta) = \sqrt{\frac{\epsilon_m - 1}{\epsilon_m} + \frac{\eta^2}{\epsilon_m \beta^2}} = \sqrt{\frac{\epsilon_m - 1}{\epsilon_m} + \frac{\mu}{\epsilon_m}}. \quad (11)$$

Approximation for surface impedance (10) is close to exact expression (11) with satisfaction of the conditions

$$|\mu| < |\epsilon_m - 1| \text{ и } |\epsilon_m| \gg 1. \quad (12)$$

The investigation of the first condition requires the knowledge of eigenvalues  $\mu$ ; we will lead it after approximations for them will be obtained.

Page 8.

In the approximate impedance setting the side wave, determined by the continuous spectrum of transverse operator under strict boundary conditions, is absent. There should be noted two limiting cases:  $\epsilon_m \rightarrow 1$  and  $h \rightarrow 0$  (with  $z = z_0 = 0$ ), when the solution of problem in a strict setting is determined by the exclusively continuous part of the spectrum, i.e., by integral term in expression (4). It is possible to show that when  $\epsilon_m \rightarrow 1$  we from (4) obtain the obvious result

$$A|_{\epsilon_m \rightarrow 1} = \frac{ih_g}{4\pi} \left( \frac{e^{ikR}}{R} + \frac{e^{ikR_1}}{R_1} \right),$$

$$R = \sqrt{r^2 + (z - z_0)^2}, \quad R_1 = \sqrt{r^2 + (z + z_0)^2},$$

and with  $h \rightarrow 0$  and  $z = z_0 = 0$

$$A|_{h \rightarrow 0} = \frac{ih_g}{2\pi} \epsilon'_m \frac{e^{ik\sqrt{\epsilon'_m} r}}{r}.$$

This speaks that the impedance approximate setting is not valid at the low altitudes of waveguide channel, i.e., first condition (12) must give the specific limitations to the height/altitude it is deep. The case of thin waveguides in detail is examined in work [8].

## § 2. Investigation of characteristic equation in a strict setting.

Let us consider characteristic equation (6) on bipinnate riemann surface for function  $\eta^* = \sqrt{\eta^2 + \beta^2(\epsilon'_m - 1)}$  (on the upper sheet  $\text{Im } \eta^* \geq 0$ , on the lower -  $\text{Im } \eta^* \leq 0$ ). The qualitative investigation of the behavior of the roots of characteristic equation in the dependence on  $\epsilon'_m$  and  $\beta$  in the general case is sufficiently complicated algebraic problem. For simplification in the investigation we will introduce the specific limitations to the value of the complex relative dielectric constant

$$\epsilon'_m = \epsilon_m + i\alpha, \quad \alpha \equiv \frac{\gamma_m}{\omega \epsilon_0} > 0.$$

First, we will consider it in the majority of the cases carried out

the inequality

$$|\varepsilon'_m| < 1,$$

in the second place, let us assume

$$\varepsilon_m > 0.$$

The roots of characteristic equation (6) on this sheet of riemann surface are arranged/located symmetrically relative to beginning of coordinates; therefore it suffices to consider equation in the lower half-plane, where  $\text{Im } \eta \leq 0$ , especially because the transformation of the duct/contour of integration in the solution of problem (3) precisely only in this half-plane occurs.

Page 9.

Initial equation (6) is reduced to two real equations

$$\frac{\sigma \sin 2\sigma - \tau \sinh 2\tau}{2(\sinh^2 \tau + \cos^2 \sigma)} = \frac{\varepsilon_m \text{Im } \eta^* - \tau \text{Re } \eta^*}{\varepsilon_m^2 + \tau^2}, \quad (13)$$

$$\sigma \tau \frac{\frac{\sin 2\sigma}{2\sigma} + \frac{\sinh 2\tau}{2\tau}}{\sinh^2 \tau + \cos^2 \sigma} = - \frac{\varepsilon_m \text{Re } \eta^* + \tau \text{Im } \eta^*}{\varepsilon_m^2 + \tau^2}, \quad (14)$$

where  $\sigma = \text{Re } \eta$ ,  $\tau = \text{Im } \eta$ . Fig. 3 depicts the lower half-plane of complex variable  $\eta$  with section/cut  $\text{Im } \eta^* = 0$  and signs  $\text{Re } \eta$  and  $\text{Im } \eta$ , which correspond to the upper sheet of riemann surface, are indicated. On the lower sheet real and imaginary parts  $\eta$  have signs, reverse/inverse indicated in the figure.

From equations (13) and (14) and that fact that on the real and imaginary axes signs  $\operatorname{Re} \eta^*$  and  $\operatorname{Im} \eta$  are identical, it follows that with the finite values  $\beta$  and  $\varepsilon_m$  the roots of equation (6) do not intersect real and imaginary axes. Further, from equation (14) taking into account the inequality

$$\frac{\sin 2\sigma}{2\sigma} + \frac{\operatorname{sh} 2\tau}{2\tau} > 0$$

follows that the roots of equation (6) can be arranged/located only the following regions of lower half-plane ( $\eta$ ):

- 1) in the fourth quadrant on the upper sheet of riemann surface;
- 2) in the fourth quadrant on the lower sheet of lower than the section/cut and its continuation;
- 3) in the third quadrant on the lower sheet of riemann surface.

Since in the third quadrant the roots are only on the lower sheet and with the change  $\beta$  and  $\varepsilon_m$  remain in this quadrant, they are not of interest for us and further we can examine equation (6) only in the fourth quadrant of plane ( $\eta$ ). Let us note the two additional general/common/total properties of the roots of equations (6), which



will be useful in the examination of their behavior, roots can intersect the upper shore of section/cut and the continuation of section/cut on the upper sheet of riemann surface and do not intersect the lower shore of section/cut on the upper sheet and the continuation of section/cut on the lower.

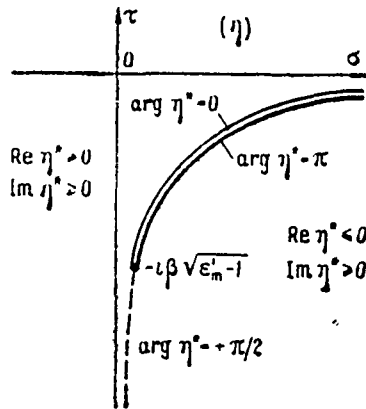


Fig 3.

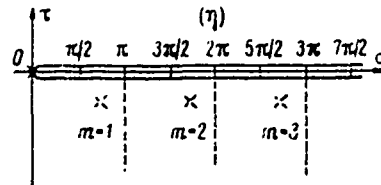


Fig. 4.

Page 10.

Further we will examine the motion of the roots of characteristic equation with that fixed/recorded  $\epsilon'_m$  and change  $\beta$  from 0 to  $\infty$  (i.e. actually so on change in altitude of waveguide  $h$ ). With  $\beta=0$  section/cut  $\text{Im } \eta^*=0$  occurs along the real axis, and characteristic equation has the following roots: dual root in the beginning of coordinates  $\eta_0^{(0)}=0$  and simple roots on the lower sheet of riemann surface

$$\eta_0^{(m)} = m\pi - \arctg \frac{l}{\epsilon'_m} \simeq m\pi - \frac{l}{\epsilon'_m}, \quad m=1; 2, 3, \dots \quad (15)$$

on the upper sheet of riemann surface roots are absent. The qualitative picture of the location of roots with  $\beta=0$  (in our old terminology [1] - points, "output") is represented in Fig. 4.

With the increase in  $\beta$  with fixed value  $\epsilon_m$  the displacement/movement of section/cut and roots of characteristic equation occurs. The equation of section/cut  $\text{Im } \eta^* = 0$  in the explicit form takes the form

$$\tau = -\frac{\beta^2 \alpha}{2\sigma}, \quad (16)$$

$$\sigma \geq \beta \sqrt{\frac{V(\epsilon_m - 1)^2 + \alpha^2 - (\epsilon_m - 1)}{2}},$$

whence it is directly evident that for  $\sigma = \text{const}$  to large  $\beta^2$  correspond the high in the modulus/module values  $\tau$ . In this case branch point  $\eta_0 = -i\beta \sqrt{\epsilon_m - 1}$  ( $\lim_{\beta \rightarrow \infty} \sqrt{\epsilon_m - 1} > 0$ ) with an increase  $\beta$  is driven out from the origin of coordinates along straight line  $\arg \eta = -\frac{\pi}{2} + \frac{1}{2} \arg(\epsilon_m - 1)$ . With  $\beta \rightarrow \infty$  the section goes away to infinity in the lower half-plane (we count  $\alpha > 0$ ). In this case the roots of characteristic equation, except one, approach real axis and have the limiting values

$$\eta_{lm}^{(m)} = \left(m + \frac{1}{2}\right)\pi.$$

According to the general/common/total properties of roots noted in the beginning of paragraph, these limiting values (point of "input") lie on the upper sheet of riemann surface. Besides the entrance points located on the real axis, equation (6) has one additional root, which exits to infinity in the lower half-plane with  $\beta \rightarrow \infty$

$$\eta_{\text{nos}} = \frac{\beta}{\sqrt{\epsilon_m + 1}}, \quad (17)$$

Moreover it is not difficult to show, utilizing (16) and (17), that it lies/rests above section/cut and its continuation, i.e., it is arranged/located also on the upper sheet of riemann surface.

Page 11.

Thus, if with  $\beta=0$  all roots are located on the lower sheet, besides one, which lies in the beginning of coordinates, then with  $\beta \rightarrow \infty$  they pass to the upper sheet, intersecting the upper shore of section/cut on it. However, before analyzing a question about the location of the roots of characteristic equation relative to section/cut, let us make some observation about the course by a line of zeros, whose equation takes the form

$$\begin{aligned} \operatorname{Im} \eta^2 \frac{1 + \epsilon_m'^2 \operatorname{tg}^2 \eta}{1 - \epsilon_m} &= 0, \\ \operatorname{Re} \eta^2 \frac{1 + \epsilon_m'^2 \operatorname{tg}^2 \eta}{1 - \epsilon_m} &> 0, \end{aligned} \quad (18)$$

since from (6) it follows

$$\beta^2 = \eta^2 \frac{1 + \epsilon_m'^2 \operatorname{tg}^2 \eta}{1 - \epsilon_m}.$$

The equation of lines of zeros in case (18) in question is much more complicated than upon the approximate impedance setting of problem [1]; therefore here we will be bounded only to qualitative

considerations and let us give the results of numerical calculations for the specific cases. Characteristic equation (6) considerably is simplified in two limiting cases

$$\begin{aligned} \text{a) } \beta \left| \sqrt{\epsilon'_m - 1} \right| &\ll |\eta|, \\ \text{b) } \beta \left| \sqrt{\epsilon'_m - 1} \right| &\gg |\eta|. \end{aligned}$$

In the case of a) the roots of equation are given by expressions (15) and is tested very small bias/displacement with the increase/growth  $\beta$  (see formula (32a)). In the case of b) equation (6) for the form is reduced to the equation in the approximate impedance setting

$$\eta t g \eta = t^*, \quad t^* = -i \delta_1^* \beta, \quad (19)$$

where

$$\delta_1^* = \frac{\sqrt{\epsilon'_m - 1}}{\epsilon_m}. \quad (20)$$

Thus, in this case (i.e. the vicinity of entrance points lines of zeros (18) are very close to lines of zeros in the approximate impedance setting with the surface impedance of the upper wall of waveguide, determined expression (20). If we count  $|\epsilon'_m| \gg 1$ , then expression (20) can be simplified and reduced to the usually utilized expression for the surface impedance of homogeneous conducting semi-infinite medium (10)

$$\delta_2^* = \frac{1}{\sqrt{\epsilon_m + 1}}. \quad (21)$$

In this case surface impedance possesses the always inductive character ( $\text{Im } \delta_{1,*} \leq 0$ ).

Page 12.

However, relations (19) and (20) are valid in region b) and when inequality  $|\epsilon_m| \gg 1$  does not occur. In this case depending on relationship/ratio  $\epsilon_m$  and  $\alpha$  surface impedance  $\delta_1^*$  can possess both inductive and capacitive ( $\text{Im } \delta_{1,*} > 0$ ) character, namely: 1)

$0 < \epsilon_m < 2$ ;  $\alpha < \sqrt{\epsilon_m(2 - \epsilon_m)} - \text{Im } \delta_1^* > 0$ , 2)  $\alpha > \sqrt{\epsilon_m(2 - \epsilon_m)} - \text{Im } \delta_1^* < 0$ , 2)  $\epsilon_m > 2$  and  $\alpha$  is arbitrary ( $\alpha > 0$ ) -  $\text{Im } \delta_{1,*} < 0$ .

Therefore, generally speaking, lines of zeros (18) in the vicinity of the entrance points located on the real axis, can behave depending on concrete/specific/actual values  $\epsilon_m$  and  $\alpha$  as lines of zeros in the approximate impedance setting, which correspond either to inductive or capacitive surface impedance. As far as line of zeros, which exits with the increase/growth  $\beta$  to infinity (it we we will call infinite line of zeros), is concerned, it with  $\epsilon_m > 0$  and  $\alpha > 0$  always exist independent of the sign of imaginary part  $\delta_1^*$  and with the large ones  $\beta$  virtually coincides with lines of zeros in the approximate impedance setting with the surface impedance  $\delta^*$ , determined by

expression (21). This line of zeros is absent only with  $\alpha=0$ , when surface impedance  $\delta_1^*$  (21) is purely active, and surface impedance  $\delta_1$  proves to be either also purely active ( $\epsilon_m > 1$ ), or purely capacitive ( $0 < \epsilon_m < 1$ ). In the case in question is sufficient large ones  $\beta$ , as we see, surface impedance of the upper wall of waveguide proves to be different for the line of zeros, which are terminated at the real entrance points  $(\delta_1^*)$ , and for line of zeros, which exits to infinity  $(\delta_1)$ . This is caused by the dependence of surface impedance (11) on the angle of incidence in the waves on the upper wall of waveguide, which must be considered, if modulus/module  $\epsilon_m$  is insufficiently great.

The study of the behavior of lines of zeros in the region, where  $\beta|\sqrt{\epsilon_m - 1}| \sim |\eta|$ , it is possible to lead actual ones only by numerical methods; therefore we in this case will make only the following observation. As can be seen from expressions (15) and Fig. 4, with  $\beta=0$  the roots of characteristic equation are arranged/located on the lower sheet of riemann surface, except one, arranged/located in the beginning of coordinates and requiring separate examination. With the increase/growth  $\beta$  the roots begin to be moved along the line of zeros, whose initial sections lie/rest on the lower sheet of lower than the section/cut and its continuation. It is not difficult to be convinced of the fact that in these sections the surface impedance  $\delta(\eta)$  (11) has inductive character. In proportion to further increase

$\beta$  the roots reach the upper shore of section/cut on the upper sheet and they emerge to the upper sheet, moreover on the upper shore of section/cut as before  $\text{Im } \delta^* < 0$ .

Page 13.

And only when section/cut departs sufficiently far from the roots, which move in turn to the entrance points along lines of zeros, surface impedance  $\delta(\eta)$  can change its character from the inductive to the capacitive. Thus, at least in the initial sections of the line of zero the imaginary part  $\delta(\eta)$  is always negative and they are arranged/located in the regions, where lie/rest lines of zeros for the inductive surface impedance in the case of the approximate impedance formulation of the problem and at which is possible the contact of lines of zeros. However, the contact of lines of zeros leads to the appearance of line of zeros, that goes to infinity, which in detail was considered in the work of the authors [1].

The phenomenon of the contact of lines of zeros is connected with the possibility of degenerating the eigenvalues of the transverse operator of problem, i.e., with the presence in the characteristic equation of multiple root. In the application/appendix to this work it is shown that at the real frequencies, examined/considered by us, the multiplicity of the roots of



characteristic equation, i.e., the algebraic multiplicity of eigenvalues, cannot exceed two, in this case the root of the second multiplicity is determined by system of equations

$$\sin \eta \cos \eta + \eta = -\frac{\cos^2 \eta}{\epsilon_m \sin \eta}, \quad (22a)$$

$$\beta^2 = \eta^2 \frac{1 + \epsilon_m \operatorname{tg}^2 \eta}{1 - \epsilon_m}. \quad (22b)$$

For the determination of the roots of the second multiplicity it is necessary actual with data  $\epsilon_m$  to solve equation (22a) and to determine its roots  $\eta_n(\epsilon_m)$  ( $n=0, 1, 2, \dots$ ). On obtained value  $\eta_n(\epsilon_m)$  one should then compute on (22b) the appropriate value of  $\beta^2$ . The degeneration of the eigenvalues (i.e. the root of the second multiplicity) occurs with similar  $\epsilon_m$  for which the obtained value of  $\beta^2$  proves to be positive. These values  $\epsilon_m$  and  $\beta^2$  correspond to the case of degeneration.

Let us recall that in the case of the approximate impedance formulation of the problem the multiple root satisfies equation [1]

$$\sin \eta \cos \eta + \eta = 0, \quad (23)$$

and value  $t = -i\delta\beta$ ,  $\delta = \frac{1}{\sqrt{\epsilon_m + 1}}$  corresponding to degeneration is determined by the expression

$$t = \eta \operatorname{tg}^2 \eta.$$

With fulfilling of inequality  $|\epsilon'_m| \gg 1$  the roots of equation (22a)  $\gamma_n$  are close to the roots of equation  $(22a) \gamma_n^{(0)}$  and the approximation formula

$$\gamma_n = \gamma_n^{(0)} - \frac{1}{2\epsilon'_m \operatorname{tg} \gamma_n^{(0)}},$$

occurs moreover in this approximation/approach relationship/ratio (22b) takes the form

$$\beta^2 = -(\epsilon'_m + 1) \gamma_n^{(0)2} \operatorname{tg}^2 \gamma_n^{(0)} + \frac{1}{\epsilon'_m + 1} \gamma_n^{(0)} \operatorname{tg} \gamma_n^{(0)}. \quad (24)$$

So that the imaginary part of  $\beta^2$  (24) would become zero with  $\operatorname{Re} \beta^2 > 0$ , the argument of value  $\epsilon'_m + 1$  ( $\gamma \equiv \arg(\epsilon'_m + 1)$ ) must satisfy the relationship/ratio

$$\gamma_n = -2\psi_n + \frac{\cos 3\psi_n}{A_n |\epsilon'_m + 1|^2}, \quad (25)$$

where

$$i\gamma_n^{(0)} \operatorname{tg} \gamma_n^{(0)} = A_n e^{i\varphi_n}.$$

In the approximate impedance setting in the right side of formula (25) the second member is absent, so that

$$\gamma_n^{\text{num}} = -2\psi_n, \quad (26)$$

and degeneration occurs for the specific arguments of value  $\epsilon'_m + 1$ , which do not depend on  $|\epsilon'_m + 1|$ . Value  $|\epsilon'_m + 1|$  affects only the value  $\beta^2$ , which corresponds to degeneration. As are shown the results of work [1], value  $\gamma_n^{\text{num}}$  (26) for the first numbers they prove to be equal to

$$\gamma_0^{\text{num}} \approx 78^\circ, \gamma_1^{\text{num}} \approx 32^\circ, \gamma_2^{\text{num}} \approx 24^\circ.$$

In strict statement when  $|\epsilon'_m| \gg 1$  the argument of value  $\epsilon'_m + 1$  (25), which corresponds to degeneration, depends on  $|\epsilon'_m + 1|$ . In this case the

degeneration at points with  $n=0$  and  $n=1$  occurs with smaller argument  $\epsilon'_m + 1$  in comparison with the impedance approximation/approach, and at points  $n \geq 2$  - with larger argument  $\epsilon'_m + 1$ .

Let us consider now the behavior of roots of characteristic equation (6) and lines of zeros in the vicinity of the entrance points and output. In the vicinity of exit point  $\eta=0$  with sufficiently small ones  $\beta$ , that satisfy the conditions

$$\beta | \sqrt{\epsilon'_m - 1} | \ll 1, \quad (27)$$

$$2\beta | \epsilon'_m \sqrt{\epsilon'_m - 1} | \ll 1, \quad (28)$$

the root of characteristic equation is given by the approximation

$$\eta = -i\beta \sqrt{\epsilon'_m - 1} \quad (29)$$

and in this approximation/approach it coincides with the point of the branching of function  $\eta^* = \sqrt{\eta^2 + \beta^2 (\epsilon'_m - 1)}$  as it follows from (29), in the vicinity  $\eta=0$  line of zeros, which emerges from this point goes along the ray/beam, which composes the angle

$$\Phi_1 = -\frac{\pi}{4} - \frac{1}{2} \operatorname{arctg} \frac{\epsilon'_m - 1}{\alpha}. \quad (30)$$

with the real axis  $\sigma$ .

Page 15.

The possible directions of line of zeros in this case are represented in Fig. 5. When  $|\epsilon'_m| \gg 1$ , with not very small ones  $\beta$ , such that

$$\beta = \frac{1}{2|\varepsilon_m|^{3/2}},$$

but simultaneously and satisfying condition  $\beta \ll |\sqrt{\varepsilon_m}|$ , it is possible to obtain for the root of characteristic equation in the region  $|\eta| < 1$  the following expression:

$$\eta = e^{-i\frac{\pi}{4}} \frac{\sqrt{\beta}}{\sqrt{\varepsilon_m}}. \quad (31)$$

In this case line of zeros is also the section of straight line, but going with respect to the real axis at the angle

$$\Phi_2 = -\frac{\pi}{4} - \frac{1}{4} \operatorname{arctg} \frac{\alpha}{\varepsilon_m}.$$

The possible directions of line of zeros in this case are represented in Fig. 6. Thus, when  $|\varepsilon_m| \gg 1$  line of zeros, which emerges from the point  $\eta=0$ , at first goes along one of the rays/beams Fig. 5, and then with the increase in  $\beta$  passes to the corresponding ray/beam Fig. 6.

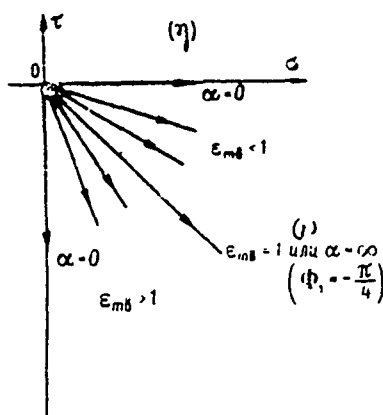


Fig. 5.

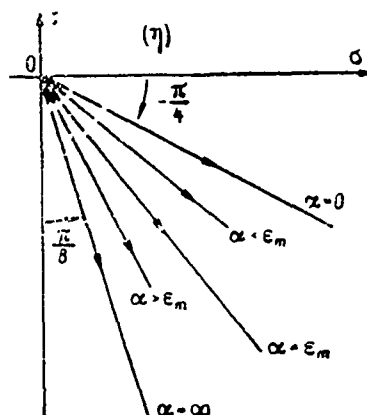


Fig. 6.

Fig. 5. Key: (1). or.

Page 16.

In the vicinity of exit points (15) with satisfaction of the conditions

$$\beta \ll \frac{m\pi}{|\epsilon'_m - 1|}, \quad \beta \ll (m\pi)^{3/2}$$

for the roots of characteristic equation it is not difficult to obtain the following approximation:

$$\gamma_{lm}^{(m)} \approx m\pi - \operatorname{arctg} \frac{l}{\epsilon_m} - \frac{l_0^2 \epsilon'_m}{2(\epsilon'_m + 1) \left[ m\pi - \operatorname{arctg} \frac{l}{\epsilon_m} \right]^2}, \quad (32)$$

which when  $|\epsilon'_m| \ll 1$  considerably is simplified

$$\gamma_{lm}^{(m)} \approx m\pi - \frac{l}{\epsilon_m} - \frac{l_0^2}{2m^2 \pi^2}. \quad (32a)$$

In this case lines of zeros in the vicinity of exit points (15) are the line segments, which go vertically down.

With an increase  $\beta$  the roots of equation (6) approach entrance points  $\eta_{\pm}^{(m)} = \left(m + \frac{1}{2}\right)\pi$  and with

$$\beta \gg \frac{\left(m + \frac{1}{2}\right)\pi}{\left|\sqrt{\epsilon_m' - 1}\right|}, \quad \beta \gg \frac{\epsilon_m'}{\left|\sqrt{\epsilon_m' - 1}\right|}$$

for them occurs the approximation

$$\eta_{\pm}^{(m)} \approx \left(m + \frac{1}{2}\right)\pi - \frac{i\epsilon_m'}{\sqrt{\epsilon_m' - 1}} \frac{\left(m + \frac{1}{2}\right)\pi}{\beta}. \quad (33)$$

Lines of zeros in vicinity of exit points go along the rays/beams, arranged/located relative to real axis  $\sigma$  at the angle

$$\Phi_j = -\frac{\pi}{2} + \operatorname{arctg} \frac{a}{b},$$

where

$$\begin{aligned} a + ib &= \sqrt{\epsilon_m - 1}, \\ a &= \sqrt{\frac{(\epsilon_m - 1)^2 + x^2 + (\epsilon_m - 1)}{2}}, \\ b &= \sqrt{\frac{(\epsilon_m - 1)^2 + x^2 - (\epsilon_m - 1)}{2}}. \end{aligned}$$

The course of lines of zeros in the vicinity of entrance point  $\eta_{\pm}^{(m)} = \left(m + \frac{1}{2}\right)\pi$  for different ones  $\epsilon_m$  and  $\alpha$  is shown in Fig. 7.

## The considerations

given

above and results make it possible to represent the dynamics of the roots of characteristic equation and the behavior of lines of zeros with different values  $\varepsilon_m$  and  $\alpha$  ( $\varepsilon_n > 0$ ,  $\alpha > 0$ ). As a whole it is possible to say that the general pattern of lines of zeros in the case of a strict formulation of the problem in question is the same and in impedance approximation/approach [1], with exception, separate parts. Corresponding line of zeros in the impedance approximation answers each line of zeros in a strict setting.

Page 17.

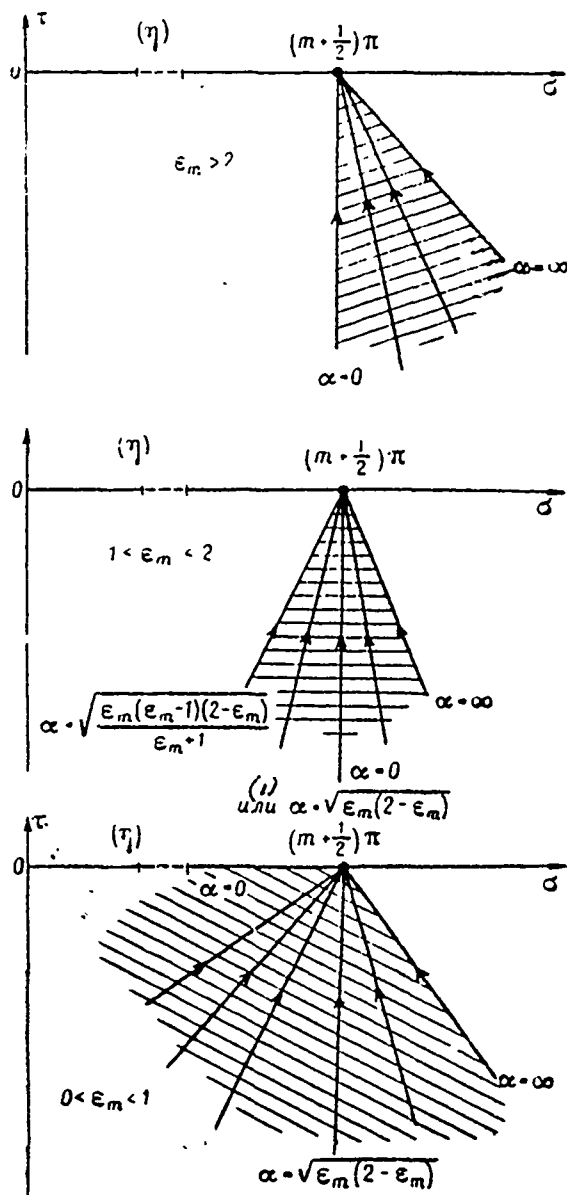


Fig. 7.



Key (1). or.

Page 18.

As earlier [1], it is possible to number the eigenvalues (roots of characteristic equation) on exit points of lines of zeros corresponding to them. Lines of zeros, arranged/located to the left and right of infinite line of zeros (17), go in opposite directions: left lines of zeros go from exit points into the adjacent entrance points which lie to the right of them, and right lines of zeros - into the adjacent entrance points which lie to the left. Exit point of infinite line of zeros depends on the argument of value  $\epsilon_m$  and in proportion to its increase it is moved at the beginning of coordinates. The displacement of exit point of this line occurs at the moment of its contact with line of zeros, which emerges from adjacent left exit point. Numerical calculations confirm the given common picture of the behavior of lines of zeros. As the illustration Fig. 8 depicts first three lines of zeros for  $\epsilon_m=1.5$  and the different values  $\alpha$ . By arrows/pointers is indicated the direction of the motion of the eigenvalues along lines of zeros with an increase  $\beta$ . With  $\alpha=0$  (dielectric waveguide) infinite line of zeros is absent and all lines of zeros go in one direction - from left to right. With  $\alpha=3$  infinite line of zeros emerges from exit point of the first mode. Line of

zeros for the zero mode goes in this case as before from left to right, and the lines of all zero modes, beginning with the third, go in the opposite direction.

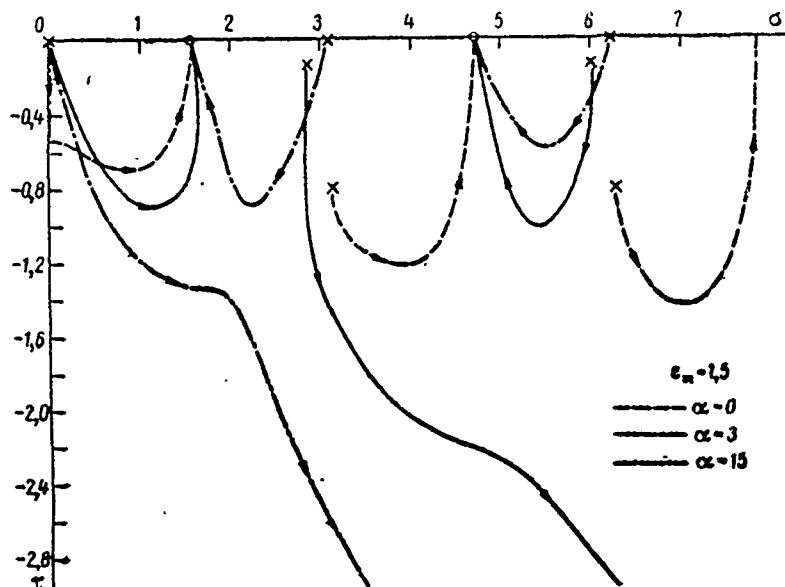


Fig. 8.

Page 19.

And finally with  $\alpha=15$  exit point of infinite line of zeros coincides with exit point of the line of zero zero modes, and all lines of zeros, except zero, go from right to left. As was already mentioned above, the displacement of exit point of infinite line of zeros is connected with the phenomenon of the contact of lines of zeros. This phenomenon for the lines of zero zero and first modes when  $\epsilon_m=1.5$  is illustrated by the results of the numerical calculations, represented in Fig. 9. Contact occurs with  $\alpha \approx 11.5$ . The argument of value  $\epsilon'_m + 1$ , which corresponds to degeneration (contact), comprises

approximately/exemplarily  $77^{\circ}45'$ , which is somewhat less than the value of the argument of this value in impedance approximation/approach ( $78^{\circ}$ ).

Although the common pattern of lines of zeros in a strict setting is close to the same in the impedance approximation/approach however on the concrete/specific/actual course of lines of zeros strict boundary conditions can exert a substantial influence, which most strongly is developed with small ones  $|\epsilon_m'|$ . Difference in the concrete/specific/actual behavior of lines of zeros upon strict and impedance formulations of the problem is connected, in particular, with the following two facts, which have already been noted above.

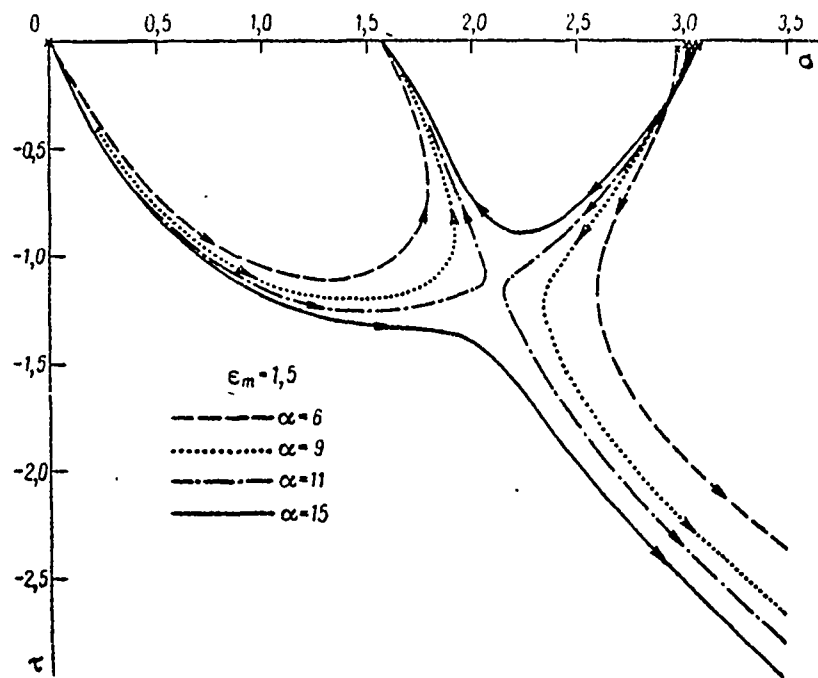


Fig. 9.

Page 20.

First, exit points of lines of zeros, besides, zero, are arranged/located upon the strict setting in contrast to the impedance not on the real axis, their removal/distance from the real axis depending on  $\epsilon_m$  and  $\alpha$  it can be considerable (so, when  $\epsilon_m=1$  and  $\alpha \rightarrow 0$  exit point go away to infinity). In the second place, in a strict setting is always an infinite line of zeros, which corresponds to the inductive surface impedance of the upper wall of waveguide in the impedance approximation/approach. However, in this case in the case

$\epsilon_m < 2$  and  $\alpha < \sqrt{\epsilon_m(2-\epsilon_m)}$  about the entrance points of line of zeros in a strict setting they go at sharp angle to the real axis (Fig. 7), which corresponds in the impedance approximation/approach to capacitive surface impedance. The latter fact leads to a noticeable change in the form of lines of zeros, especially lines of zeros with the large numbers. Fig. 10 shows lines of zeros for  $\epsilon_m = 0.1$  and different  $\alpha$ , that correspond to the ninth and tenth normal waves. Results given in this figure, and also results in Fig. 8 and 9 sufficiently clearly illustrate the fundamental special features/peculiarities of lines of zeros in the case of a strict formulation of the problem in question.

Above we examined the course of lines of zeros, without being interested, on what sheet of riemann surface zero are arranged/located. Let us pause now at this question, since it has vital importance in view of the fact that in the series/row of normal waves for the solution of problem in the form (4) enter only the terms, which correspond to the roots of the characteristic equation, which are arranged/located on the upper sheet of riemann surface in the lower half-plane. Let us begin from the examination of zero root, which corresponds to zero mode and which is found with  $\beta=0$  in the beginning of coordinates ( $\eta_0^{(0)}=0$ ).

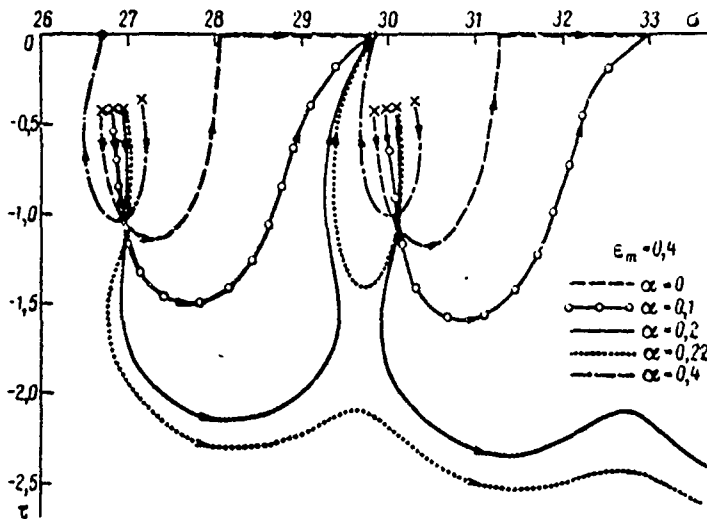


Fig. 10.

Page 21.

With small  $\beta$ , that satisfy inequalities (27) and (28), this root lies/rests at the vicinity of the point of branching of function  $\eta^*$  (29). Utilizing equation (6), it is not difficult to ascertain that it is located on the upper sheet of Riemann surface, if occurs the inequality

$$\epsilon_m (\epsilon_m - 1) < \alpha^2, \quad (34)$$

also, on the lower sheet with the reverse/inverse inequality

$$\epsilon_m (\epsilon_m - 1) > \alpha^2. \quad (35)$$

For the zero root with small ones  $\beta$  it is possible to obtain the more exact expression than (29), applying the method of successive

approximations for solving equation (6), which in the case  $|\eta| \ll 1$  in question takes the form

$$\eta^2 = -\beta^2 (\varepsilon'_m - 1) - \varepsilon_m'^2 \eta^4.$$

In the first approximation, we obtain

$$\eta^{(0)2} = -\beta^2 (\varepsilon'_m - 1) - \beta^4 \varepsilon_m'^2 (\varepsilon'_m - 1)^2.$$

From this expression the following relationship/ratio for the product of the real and imaginary parts  $\eta^{(0)} = \sigma^{(0)} + i\tau^{(0)}$ :

$$2\sigma^{(0)}\tau^{(0)} = -\beta^2 \alpha - 4\beta^3 \alpha (\varepsilon_m - 1) [\varepsilon_m (\varepsilon_m - 1) - \alpha^2]. \quad (36)$$

ensues. Comparing relationship/ratio (36) with the equation of section/cut and its continuation

$$2\sigma_p \tau_p = -\beta^2 \alpha,$$

it is not difficult to arrive at the following conclusions relative to the mutual location of root  $\eta^{(0)}$  and section/cut or its continuation (Fig. 11) in the case of small ones  $\beta$ :

when  $0 < \varepsilon_m < \frac{1}{2}$  root is arranged/located on the upper sheet of riemann surface in region (1c), limited by positive real semi-axis, by the negative imaginary semi-axis, by section/cut and by its continuation;

when  $\frac{1}{2} < \varepsilon_m < 1$  root is arranged/located on the upper sheet in



region (2c), which is arranged/located in the fourth quadrant to the right and are lower than the section/cut its continuations;

$\varepsilon_m > 1$  and fulfilling of inequality (34) root is arranged/located also in region (2c);

with  $\varepsilon_m > 1$  and fulfilling of inequality (35) the root is located on the lower sheet in region (2m).

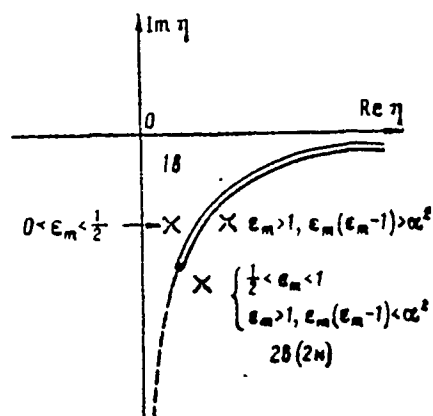


Fig. 11.

Page 22.

In the latter case with the increase/growth  $\beta$  zero root passes from the lower sheet of riemann surface to the upper, intersecting with certain value  $\beta = \beta_{kp}^{(0)}$  section/cut  $\text{Im } \eta^* = 0$ . Value  $\beta_{kp}^{(0)}$  depends on modulus/module and argument of value  $\varepsilon'_m = \rho e^{i\varphi}$  ( $\rho = \sqrt{\varepsilon_m^2 + \alpha^2}$ ,  $\varphi = \arctg \frac{\alpha}{\varepsilon_m}$ ). In order to estimate value  $\beta_{kp}^{(0)}$ , let us consider for simplicity the case, when  $|\varepsilon'_m| = \rho \gg 1$ , and we will use approximation formula (31), valid with

$$\sqrt{\rho} \gg \beta \gg \frac{1}{2\rho^{3/2}}.$$

Based on this formula, it is not difficult to show that in case (35) interesting us for  $\beta_{kp}^{(0)}$  the approximation

$$\beta_{kp}^{(0)} = \frac{1}{2\rho^{3/2} \ln \frac{\rho}{\alpha}}. \quad (37)$$

occurs. The obtained expression for  $\beta_{kp}^{(0)}$  is correct not with very

small<sup>1</sup>  $\phi$ , such that

$$\sin \frac{\phi}{2} \approx \frac{1}{2\phi^2}.$$

FOOTNOTE <sup>1</sup>. In this case  $\phi$  does not exceed  $\pi/4$  (we count  $\epsilon_m \approx 1$ ), since otherwise zero root is found on the upper sheet of Riemann surface already with as small as desired  $\beta$ . ENDFOOTNOTE.

With the decrease of imaginary part  $\epsilon_m'$ , by decrease  $\phi$ , value  $\beta_{kp}^{(0)}$  grows/rises also with certain sufficiently small  $\phi$  expression (37) proves to be wrong. In the case of small ones  $\phi$  the intersection of the roots of section/cut can be investigated, relying on approximation formula (33), which for zero root ( $m=0$ ) when  $|\epsilon_m| \gg 1$  takes the following form:

$$\eta_0^{(0)} \approx \frac{\pi}{2} - \frac{i\pi \sqrt{\epsilon_m'}}{2\phi}. \quad (38)$$

Fulfilling of the inequality

$$\beta \gg \sqrt{\rho} = |\sqrt{\epsilon_m'}|.$$

is applicability the condition for this approximation. from expression (38) it follows that the root intersects section/cut with

$$\beta = \beta_{kp}^{(0)} \approx \left[ \frac{\pi^2}{4\sqrt{\rho} \sin \frac{\phi}{2}} \right]^{1,3}. \quad (39)$$

Formula (39) is valid for sufficiently small ones  $\phi$ , which satisfy the condition

$$\sin \frac{\phi}{2} < \frac{\pi^2}{4\phi^2}.$$

Page 23.

Thus, from expressions (37) and (39) it ensues that value  $\beta_{kp}^{(m)}$ , with which zero root transits from the lower sheet of riemann surface to the upper, grows/rises with the decrease  $\alpha$  (~~t.e.~~ <sup>i.e.</sup>  $\phi$ ) and it approaches infinity with  $\alpha \rightarrow 0$ .

As far as other roots of the characteristic equation (6), arranged/located in the fourth quadrant, are concerned, they with  $\beta=0$  lie/rest on the lower sheet of Riemann surface, and with the increase/growth  $\beta$  in the case  $\alpha > 0$  just as zero root, they pass from the lower sheet to the upper. Those corresponding to these roots of value  $\beta_{kp}^{(m)}$ , with which the roots intersect section/cut, can be determined, utilizing approximations (32a) (32b) and (33). Thus, in the case  $\rho \gg 1$  and  $\sin \phi \gg 1/\pi\rho$  for  $\beta_{kp}^{(m)}$  occurs the following approximation:

$$\beta_{kp}^{(m)} = \sqrt{\frac{2m\pi}{\rho^2 \lg \phi}}, \quad (40)$$

from which it follows that the roots intersect section/cut with different ones  $\beta_{kp}^{(m)}$ , whose value grows/rises with an increase in number  $m$ . At the same time in the case not of not very small ones in question  $\phi$  zero root appears at the upper sheet with the

increase/growth  $\beta$  earlier than the first, which is evident from expressions (37) and (40).

Thus, with the finite values of  $\beta$  on the upper sheet of riemann surface is located a finite number of roots of characteristic equation (6), i.e., the discrete spectrum of the transverse operator of problem consists of a finite number of isolated points (it is intended compare  $\epsilon_m > 0$ ). With small ones  $\beta$ , that satisfy relationships/ratios (27) and (28), the discrete spectrum more proves to be empty, if the properties of the upper medium, which limits waveguide, are subordinated to condition (35). Let us note that in the case  $\alpha=0$  and  $\epsilon_m > 1$  the discrete spectrum is absent with any values  $\beta$ . With  $\alpha > 0$  a number of points of discrete spectrum depends on the height/altitude of waveguide (or value  $\beta = kh$ ) and increases with the increase/growth  $\beta$ . The fact of the finiteness of a number of points of discrete spectrum was not noticed in preceding/previous investigations [3], [4], although for the thin waveguides it can play a significant role during the representation of field in the form of the series/row of normal waves.

§ 3. Some generalities about the representation of the solution of problem in the form of the series/row of normal waves.

As it was shown in the preceding/previous paragraph, the

discrete spectrum of the transverse operator of problem when consists of a finite number of isolated points, i.e., in the  $\epsilon_m > 0$  decomposition of solution in the form (4) a finite number of normal waves enters. For the evaluation/estimate of number N of normal waves in the case of  $|\epsilon'_m| \gg 1$  and  $\arg \epsilon'_m \gg \frac{1}{|\epsilon'_m|}$  it is possible to use approximation formula (40).

Page 24.

When the conduction currents in the upper medium considerably exceed bias currents, from formula (40) we find

$$N \approx \left[ \frac{3600 \sigma_u h^2}{\epsilon_m \epsilon_u f} \right], \quad (41)$$

where the brackets indicate whole part of the number, included in them<sup>1</sup>.

FOOTNOTE <sup>1</sup>. Let us recall that  $\sigma_u$  is the conductivity of the media, which limits waveguide on top. ENDFOOTNOTE.

If the height of waveguide is 70 km, and the conductivity of upper medium is equal to  $10^{-6}$  1/ohm·m, then an Earth-ionosphere in the range of the superlong waves corresponds to the effective properties of waveguide channel in the daytime conditions for propagation, then a number of normal waves at the frequency of 10 kHz proves to be

approximately/exemplarily equal to 180. In this case the fact that a number of normal waves is certain, does not have vital importance, since a number of normal waves, necessary for describing the field at the distances from the source, large several hundred kilometers, does not exceed ten. So that the number of normal waves with the properties of upper medium indicated would compose several ones, the height/altitude of waveguide channel must not exceed 10 km. The finiteness of a number of normal waves can prove to be essential for the thin waveguides or when the medium, which limits waveguide on top, is low-loss dielectric. In these cases in the decomposition of the solution of problem (4) the integral along the continuous spectrum plays a noticeable role.

The fact of the finiteness of a number of the eigenvalues of the non-self-adjoint differential operator of the second order, assigned on the semi-axis, is sufficiently familiar and investigated in the series/row of mathematical works [9] when the coefficients of differential expression satisfy the specified conditions. However, obtained in these works the results are not directly applicable to the examined by us case, since there are not satisfied the utilized in them conditions. The problem investigated by us shows that the finiteness of a number of eigenvalues can occur, also, under the wider assumptions about the behavior of coefficients of differential expression.

Expansion (4) of the solution of problem encompasses the series of the normal waves of those corresponding to the eigenfunctions of transverse operator, and integral on the duct/contour  $G$  (Fig. 2), which is integral along the continuous spectrum of this operator. It is here interesting to note the following fact.

Page 25.

If we examine the solution of problem only in the interval  $0 \leq z \leq h$  (expansion (4) corresponds to precisely this case), then the duct/contour of the integration it is possible to deform and to transfer it into the duct/contour, whose part will be arranged/located on the lower sheet of riemann surface for the function  $\eta^*$  (for example, duct/contour  $G'$  in Fig. 12, where by solid line it is shown the part of the duct/contour, arranged, located on the upper sheet, and by dotted line - on the lower sheet). During this deformation of the duct/contour of integration  $G$ , which can be required, for example, for computing the integral along the continuous spectrum (side wave) with the help of the method of steepest descent, they will, generally speaking, intersect the pole of the integrands, which correspond to the roots of characteristic equation, arranged/located on the lower sheet of riemann surface. as



a result in expansion (4) together with the series of normal waves will appear the series/row of deductions in these poles, which we will call the series of quasi-normal waves, since the transverse functions, entering into them, are not the eigenfunctions of transverse operator. The transverse functions of quasi-normal waves satisfy differential equation for the eigenfunctions and boundary conditions with  $z=0$  and  $z=h$ , but they do not satisfy boundary condition at infinity - they exponentially increase with  $z \rightarrow \infty$ . A number of quasi-normal waves in the decomposition of the solution of form (4) can be arbitrary, including infinite (but calculating), depending on the concrete/specific/actual selection of duct/contour  $G'$ . During the described deformation of duct/contour  $G$  into the duct/contour  $G'$  the field of the side wave (integral along the continuous spectrum) is represented in the form of the series/row of quasi-normal waves and integral on the duct/contour  $G'$ , which subsequently [8] we will call sky wave when duct/contour  $G'$  corresponds to the duct/contour of the fastest descent, passing through points  $\gamma_1 = -i\beta \sqrt{\varepsilon_m' - 1}$ .

Let us pause now at the properties of normal wave, which corresponds to the eigenvalue, arranged/located on infinite line of zeros. The properties of other normal waves are sufficiently well studied in the series/row of works [3-6]. As it was shown in the

preceding/previous paragraph, among the eigenvalues of transverse operator with  $\alpha > 0$  is always one value, which is arranged/located on line zero, which exits to infinity with  $\beta \rightarrow \infty$ . With satisfaction of condition  $\left| \operatorname{Im} \frac{\beta}{\sqrt{\epsilon_m - 1}} \right| > 1$  this eigenvalue is given by approximation (17).

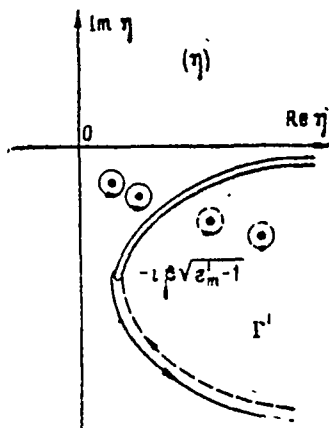


Fig. 12.

Page 26.

However, for determining the excitation coefficient of the corresponding normal wave approximation (17) proves to be insufficient and it must be made more precise. Utilizing during the solution of equation (6) a method of successive approximations in the region  $|\text{Im } \eta| > 1$ , it is not difficult to obtain in the first approximation, the following expression for the eigenvalue in question:

$$\eta_{\text{mos}} \approx \frac{\beta}{\sqrt{\epsilon_m + 1}} + \frac{2\epsilon_m^{1/2}}{(\epsilon_m^{1/2} - 1)\sqrt{\epsilon_m + 1}} e^{-\frac{2\beta}{\sqrt{\epsilon_m + 1}}}$$

The excitation coefficient of this normal wave in this case proves to be equal to

$$A_{\text{nos}} \approx \frac{4i\tilde{\epsilon}_m'^2}{(\epsilon_m'^2 - 1)\sqrt{\epsilon_m' + 1}} e^{-\frac{2i\delta}{\sqrt{\epsilon_m' + 1}}},$$

and the part of the vector potential, which corresponds to it, in wave zone ( $kr \gg 1$ ) when  $|\epsilon_m'| \gg 1$  takes the form

$$A_{\text{nos}} \approx \frac{i h_g}{2\pi r} e^{ikr} \sqrt{\pi sr} e^{-sr - 2i\delta} f_{\text{nos}}(z) f_{\text{nos}}(z_0),$$

where are introduced the following designations:

$$s = \frac{ik\delta^2}{2}, \quad \delta = \frac{1}{\sqrt{\epsilon_m' + 1}}.$$

With  $z = z_0 = h$  vector potential  $A_{\text{nos}}$  in this approximation/approach is given by the expression

$$A_{\text{nos}}|_{z=z_0=h} \approx \frac{i h_g}{2\pi r} e^{ikr} \sqrt{\pi sr} e^{-sr},$$

which in the form coincides with the ground wave of Tsennek in the problem of Sommerfield [10] about the propagation of the electromagnetic waves above the flat surface with the source and the receiver, arranged/located on it. Value  $sr$  is the numerical distance, introduced in this problem. High-altitude factors  $f_{\text{nos}}(z)$  of the considered/examined normal wave actually exponentially grow/rise with an increase in altitude, which indicates the fact that its energy in essence is concentrated in the vicinity of the upper wall of waveguide. in view of these facts we call this normal wave surface.

At conclusion of this paragraph let us consider applicability conditions for impedance of approximation during the determination of

the eigenvalues of transverse operator. As already mentioned in the first paragraph, these conditions are determined by inequalities (12), the first of which can be rewritten as follows, utilizing a relationship/ratio  $\eta = \beta/\mu$ :

$$|\eta| \ll \beta^2 |\epsilon'_m - 1|. \quad (42)$$

Page 27.

If we utilize for  $\eta$  approximation (31), then it is not difficult to be convinced of the fact that inequality (42) for the eigenvalue of zero mode in the case  $|\epsilon'_m| \gg 1$  is fulfilled under the condition

$$\beta \gg \frac{1}{|\epsilon'_m|^{3/2}}. \quad (43)$$

The eigenvalues of other normal waves, except one, corresponding to infinite line zero, possess the real part, which exceeds several times imaginary, as is evident from the results of the numerical calculations, represented in Fig. 8-10. In this case the real part of the eigenvalue of  $m$ -th normal wave is of the order  $m\pi$ , so that inequality (42) in this case takes the form

$$\beta \gg \frac{m\pi}{|\epsilon'_m|} \quad (m = 1, 2, 3, \dots). \quad (44)$$

However, as far as the eigenvalue, which lies on infinite line of zeros, is concerned, as it follows from approximation (17),

inequality (42) occurs, if  $|\varepsilon'_m| \gg 1$ . Thus, applicability conditions for the impedance approximation/approach for eigenvalues are determined by inequality  $|\varepsilon'_m| \gg 1$  and inequalities (43) and (44) respectively for the zero and following normal waves. With satisfaction of these conditions the excitation coefficients of normal waves in impedance approximation/approach (8) with the high degree of accuracy coincide with the excitation coefficients in strict setting (5). Otherwise impedance approximation/approach leads to the essential difference in the properties of the normal waves in comparison with the strict setting. Thus, for instance, for the zero mode in the case of the thin waveguide, when is fulfilled inequality  $4\beta^2 |\varepsilon'_m (\varepsilon'_m - 1)| \ll 1$ , upon a strict setting the eigenvalue is determined by approximation formula  $\eta_{0p}^{(0)} \approx -i\beta \sqrt{\varepsilon'_m - 1}$ , whereas in the impedance approximation/approach you have  $\eta_{0mn}^{(0)} \approx \sqrt{-i\beta \delta}$ ,  $\delta = \frac{1}{\sqrt{\varepsilon'_m + 1}}$ . In this case an excitation coefficient of zero mode in a strict setting proves to be equal to  $\Lambda_0^{(0)p} \approx \beta^2 \varepsilon'_m (\varepsilon'_m - 1)$ ,  $|\Lambda_0^{(0)p}| \ll 1$ , and in impedance approximation/approach  $\Lambda_0^{(0)p} \approx \frac{1}{2}$ .

Page 28.

Inequalities (43) and (44), are determined the applicability of impedance approximation/approach, superimpose definite requirements for the height/altitude of waveguide. For the thin waveguides the impedance approximate setting can prove to be unsuitable, in spite of fulfilling of inequality  $|\varepsilon'_m| \gg 1$ . In the case of waveguides with the

sufficiently high altitude the impedance approximation/approach is inapplicable for the normal waves of high order (with the high value of  $m$ ); however, these normal waves possess high attenuation, since they prove to be those not running, and are unessential for the description fields already at comparatively small distances from the source.

#### APPENDIX.

Investigation of the multiplicity of the roots of characteristic equation.

Let us show that characteristic equation (6) does not have roots of the third multiplicity at the real frequencies (i.e. with  $\beta^2 > 0$ ). The roots of the second multiplicity must satisfy the equations

$$i\epsilon'_m \eta \operatorname{tg} \eta = \sqrt{\eta^2 + \beta^2 (\epsilon'_m - 1)}, \quad (1n)$$

$$i\epsilon'_m \operatorname{tg} \eta + i\epsilon'_m \eta = -\sqrt{\eta^2 + \beta^2 (\epsilon'_m - 1)} \operatorname{tg} \eta + \frac{\eta}{\sqrt{\eta^2 + \beta^2 (\epsilon'_m - 1)}}. \quad (2n)$$

For the roots of the third multiplicity must be performed one additional equation

$$2i\epsilon'_m = -\frac{2\eta \operatorname{tg} \eta - 1}{\sqrt{\eta^2 + \beta^2 (\epsilon'_m - 1)}} - \frac{\eta^2}{[\eta^2 + \beta^2 (\epsilon'_m - 1)]^{3/2}}. \quad (3n)$$

eliminating  $\sqrt{\eta^2 + \beta^2 (\epsilon'_m - 1)}$  from (2n) with the help of (1n) expressing  $\beta^2$  from (1n) through  $\epsilon'_m$  and  $\eta$ , we come to two equations for the twofold

roots

$$\sin \eta \cos \eta + \eta = - \frac{\cos^2 \eta}{\epsilon_m^2 \sin \eta}, \quad (4n)$$

$$\beta^2 = \eta^2 \frac{1 + \epsilon_m^2 \eta^2}{1 - \epsilon_m^2}. \quad (5n)$$

If we now exclude  $\sqrt{\eta^2 + \beta^2(\epsilon_m^2 - 1)}$  from (3n) with the help of (1n) and with the help of (4n), then equation (3n) is reduced to the following form:

$$3 \sin \eta \cos \eta + \eta (1 + 2 \sin^2 \eta) = 0 \quad (6n)$$

utilizing this equation, it is not difficult from equations (4n) and (5n) to find the expressions for  $\epsilon_m^2$  and  $\beta^2$  which correspond to the roots of the third multiplicity

$$\epsilon_m^2 = \frac{2 - \cos 2\eta}{1 - \cos 2\eta}, \quad \beta^2 = - \frac{27}{4} \frac{\epsilon_m^2 + 1}{\epsilon_m^2}. \quad (7n)$$

Thus, the roots of the third multiplicity are the roots of equation (6n), which can be rewritten in the following form:

$$F(\xi) = 3 \sin \xi + \xi (2 - \cos \xi) = 0, \quad \xi = 2\eta, \quad (8n)$$

but values  $\epsilon_m^2$  and  $\beta^2$  corresponding to them are determined by expressions (7n). Now it is necessary to find the roots of equation (8n) and corresponding to them values  $\epsilon_m^2$  and  $\beta^2$ . Equation (8n) is reduced to two real equations

$$3 \sin x \operatorname{ch} y + 2x - x \cos x \operatorname{ch} y - y \sin x \operatorname{sh} y = 0, \quad (9n)$$

$$3 \cos x \operatorname{sh} y + 2y - y \cos x \operatorname{sh} y + x \sin x \operatorname{sh} y = 0, \quad (10n)$$

where  $\xi = x + iy$ .



Page 29.

Roots of equation (8n) are arranged/located symmetrically relative to x and y axes; therefore it suffices to consider them only in the fourth quadrant of plane ( $\xi$ ).

Equation (8n) has, in the first place, a root  $\xi=0$  ( $x=0$ ,  $y=0$ ), for which  $|\epsilon'_m|=\infty$  and  $\beta^2=0$ . This root does not represent for us interest. In the second place, equation (8n) has the imaginary root, which satisfies equation (10n) with  $x=0$

$$3 \frac{\operatorname{sh} y}{y} = \operatorname{ch} y - 2. \quad (11n)$$

The numerical solution of equation (11n) leads to the following value of this root and values  $\epsilon'_m$  and  $\beta^2$  corresponding to it:

$$\begin{aligned} \xi_0 &= -13,436; \quad \epsilon'_{m0} = 0,965; \quad \beta_0^{(+)^2} = -1,530; \\ \epsilon'_{m0} &= -0,965; \quad \beta_0^{(-)^2} = -0,272. \end{aligned}$$

On the real axis ( $y=0$ ,  $x>0$ ) equation (8n), which is led to the form

$$2 + 3 \frac{\operatorname{sh} x}{x} - \cos x = 0,$$

does not have solutions.

For the localization of the position of complex roots of

equation (8n) and explanation of their multiplicity it is possible to use the Cauchy theorem and a number of roots of regular function [11]. Applying this theorem to function  $F(\xi)$  in the regions of complex plane ( $\xi$ ), limited by the sections of straight lines  $y=0$ ,  $y=-C(C \gg 1)$ ,  $x=C_1$ ,  $x=C_2$ , is not difficult to show that the roots of equation (8n), besides those noted above, are arranged/located in the bands

$$\left(2k - \frac{1}{2}\right)\pi < y < 2k\pi \quad (k=1, 2, 3, \dots).$$

moreover all roots are simple. During the solution of system of equations (9n)-(10n) it is expedient instead of  $x$  to introduce a new variable

$$\epsilon_k = 2k\pi - x,$$

which varies in an interval from 0 to  $\frac{\pi}{2}$ . The system of (9n)-(10n) equation is convenient to record in the form, suitable for using this method of successive approximations,

$$\begin{cases} \operatorname{ch} y_k = 2 + 4 \frac{\sin^2 \frac{\epsilon_k}{2}}{\cos \epsilon_k} - (3 \operatorname{ch} y_k - y_k \operatorname{sh} y_k) \frac{\operatorname{tg} \epsilon_k}{x_k}, \\ \sin \epsilon_k = \frac{3}{x_k} - \frac{6}{x_k} \sin^2 \frac{\epsilon_k}{2} + \frac{y_k}{\operatorname{sh} y_k} (3 \operatorname{ch} y_k - y_k \operatorname{sh} y_k) \frac{\sin \epsilon_k}{x_k^2}, \\ x_k = 2k\pi - \epsilon_k. \end{cases} \quad (12n)$$

Since  $x_k \gg 1$  and  $2k\pi \gg \epsilon_k$ , in the zero approximation we obtain the the following expressions for the roots of equations(8n):

$$\begin{aligned} \epsilon_k^{(0)} &= x_k^{(0)} + i y_k^{(0)}, \quad x_k^{(0)} = 2k\pi - \epsilon_k^{(0)}, \\ \epsilon_k^{(0)} &= \frac{3}{2k\pi}, \\ \operatorname{ch} y_k^{(0)} &= 2, \quad y_k^{(0)} = y^{(0)} = -1,3170. \end{aligned} \quad (13n)$$

(14n)

Page 30.

Table I.

$k$	$y_k$	$\epsilon_k$	$\sigma_k$	(1) $\text{Re } \epsilon_{kk} (\tau)$ (точн.)	(2) $\text{Re } \epsilon_{kk} (+)$ (прибл. (15 п))	(1) $\text{Im } \epsilon_{kk} (-)$ (точн.)	(2) $\text{Im } \epsilon_{kk} (-)$ (прибл. (15 п))
1	-1,280	0,5173	0,4775	-0,7822	-0,7990	0,4594	0,4870
2	-1,309	0,2432	0,2387	-0,5066	-0,5098	0,3954	0,3995
3	-1,314	0,1605	0,1592	-0,4001	-0,4013	0,3398	0,3412
4	-1,315	0,1199	0,1194	-0,3403	-0,3410	0,3013	0,3020
5	-1,316	0,09576	0,09549	-0,3012	-0,3015	0,2733	0,2736
6	-1,316	0,07972	0,07958	-0,2729	-0,2731	0,2517	0,2519
7	-1,316	0,06830	0,06821	-0,2512	-0,2514	0,2344	0,2346
8	-1,317	0,05975	0,05969	-0,2341	-0,2342	0,2203	0,2205
9	-1,317	0,05310	0,05305	-0,2200	-0,2201	0,2085	0,2086
10	-1,317	0,04778	0,04775	-0,2081	-0,2082	0,1983	0,1984
11	-1,317	0,04343	0,04341	-0,1980	-0,1981	0,1895	0,1896
12	-1,317	0,03981	0,03979	-0,1894	-0,1894	0,1819	0,1812
13	-1,317	0,03674	0,03673	-0,1817	-0,1817	0,1750	0,1750
14	-1,317	0,03412	0,03411	-0,1748	-0,1748	0,1689	0,1689
15	-1,317	0,03184	0,03183	-0,1687	-0,1687	0,1633	0,1633
16	-1,317	0,02985	0,02984	-0,1631	-0,1631	0,1583	0,1583
17	-1,317	0,02809	0,02809	-0,1581	-0,1581	0,1537	0,1537
18	-1,317	0,02653	0,02653	-0,1535	-0,1535	0,1494	0,1494
19	-1,317	0,02513	0,02513	-0,1494	-0,1494	0,1456	0,1456
20	-1,317	0,02388	0,02388	-0,1455	-0,1455	0,1420	0,1420

Key: (1). (it is precise.). (2). (appr. (15 p)).

Page 31.

Table II.

k	$\operatorname{Re} \beta_k^{(-)2}$ (1) (точн.)	$\operatorname{Re} \beta_k^{(-)2}$ (прибл. (16n)) (2)	$\operatorname{Im} \beta_k^{(+ )2}$ (точн.) (1)	$\operatorname{Im} \beta_k^{(-)2}$ (прибл. (16n)) (2)	$\operatorname{Re} \beta_k^{(-)2}$ (точн.) (1)	$\operatorname{Re} \beta_k^{(-)2}$ (прибл. (17n)) (2)	$\operatorname{Im} \beta_k^{(-)2}$ (точн.) (1)	$\operatorname{Im} \beta_k^{(-)2}$ (прибл. (17n)) (2)
1	5,036	—	0,5666	—	5,454	—	— 17,51	—
2	24,60	—	4,604	—	45,23	—	— 41,90	—
3	60,18	—	11,58	—	108,3	121,8	— 68,40	— 61,72
4	112,8	—	21,13	—	194,3	208,7	— 97,31	— 89,10
5	182,2	—	32,85	—	302,0	317,7	— 128,2	— 118,9
6	269,4	—	46,58	—	431,9	448,6	— 161,2	— 150,8
7	374,8	—	62,27	—	584,4	601,1	— 196,2	— 184,6
8	497,6	—	79,63	—	757,7	775,3	— 232,7	— 220,2
9	638,2	—	98,59	—	958,3	970,8	— 270,9	— 257,6
10	798,1	—	119,3	—	1170	1188	— 310,7	— 296,5
11	975,4	962,7	141,2	126,2	1407	1426	— 352,0	— 336,9
12	1168	1157	164,3	148,9	1662	1685	— 394,0	— 378,8
13	1382	1371	189,2	172,9	1943	1965	— 438,0	— 422,0
14	1615	1602	215,2	198,3	2245	2267	— 483,4	— 466,5
15	1865	1852	242,1	225,0	2566	2589	— 530,3	— 512,4
16	2138	2120	271,4	252,9	2913	2933	— 577,9	— 559,4
17	2425	2407	301,0	282,0	3277	3297	— 626,8	— 607,6
18	2734	2713	332,1	312,3	3666	3683	— 677,2	— 657,1
19	3054	3037	363,0	343,6	4064	4088	— 728,1	— 707,6
20	3398	3380	396,0	376,1	4492	4515	— 780,3	— 759,2

Key: (1). (it is precise.). (2). (appr. p).

Page 33.

In the same approximation/approach of value  $\beta_m$  and  $\beta^2$ , that correspond to triple root, are given by the formulas

$$\epsilon_{mk}^{(+), (-)} = \pm \sqrt{\frac{3\sqrt{3}}{4k\pi}} \left[ -\left(1 + \frac{\sqrt{3} - y^{(0)}}{4k\pi}\right) + i \left(1 - \frac{\sqrt{3} - y^{(0)}}{4k\pi}\right) \right], \quad (15n)$$

$$\beta_k^{(+)^2} = k^2 \pi^2 \left\{ 1 - \sqrt{\frac{3\sqrt{3}}{4k\pi}} + i \left[ \sqrt{\frac{3\sqrt{3}}{4k\pi}} - \frac{\sqrt{3} - y^{(0)}}{k\pi} \right] \right\}, \quad (16n)$$

$$\beta_k^{(-)^2} = k^2 \pi^2 \left\{ 1 + \sqrt{\frac{3\sqrt{3}}{4k\pi}} - i \left[ \sqrt{\frac{3\sqrt{3}}{4k\pi}} + \frac{\sqrt{3} - y^{(0)}}{k\pi} \right] \right\}. \quad (17n)$$

In Table I are given values  $y_k$  and  $\epsilon_k$  obtained by the numerical solution of system of equations (12n), and values  $\epsilon_k^{(0)}$  (13n), and also precise values  $\epsilon_{mk}^{(+)}$  and equations (8n) calculated by approximation formula (15n) for the first twenty roots. As can be seen from the given numerical results, the approximation formulas for  $y_k$ ,  $\epsilon_k$  and  $\epsilon_{mk}$  provide high accuracy already with not very high values of  $k$  (order of several units). The results of the numerical calculations of values  $\beta_k^{(+), (-)^2}$  are represented in Table II. The accuracy of approximation formulas (16n) (17n) for  $\beta_k^2$ , especially for  $\text{Im} \beta_k^{(+)^2}$ , are much lower than formulas (13n)-(15n) for  $\epsilon_k$ ,  $y_k$ ,  $\epsilon_{mk}$ , however, it proves to be not less than several percentages with  $k=20$ . From the given results of numerical calculations for  $k=1-20$  and from approximation formulas (16n) (17n) for  $k>20$  it follows that for the roots of the third multiplicity of initial characteristic equation (6) value  $\mu^-$  has complex value. Consequently, with  $\beta^2 > 0$  (i.e. real  $k=\omega/c$ ) the multiplicity of the roots of characteristic equation cannot exceed two.

## REFERENCES.

1. G. I. Makarov, V. V. Novikov. In the collection of the "problem of diffraction and propagation of waves", iss. III, page 34, publ. of LGU, 1968.

2. G. ~~I~~. Makarov, V. V. Novikov, S. T. Rybachek. In the collection "Problems of diffraction and propagation of waves", iss. IX, page 3, publ. of LGU, 1969.

3. P. A. ~~Ryzain~~ <sup>Ryazin</sup>, L. M. Brekhovskikh. Izv. of the AS USSR, ser. phys., 10, 285, 1946.

4. L. M. Brekhovskikh. Waves in the laminar media. Publ. of the AS USSR. M., 1957.

5. K. G. Budden. Phil. Mag., 42, 1, 1951; 43, 1179, 1952.

6. J. P. Wait. Trans. IRE, AP-1, N 1, 9, 1953; AP-2, N 4, 144, 1954

7. P. Ye. Krasnushkin. Method of normal waves in application to the problems of remote radio communications. Publ. of MGU, 1947.

8. G. I. Makarov, V. V. Novikov. this collector/collection, page 00.

9. M. A. Naymark. Linear differential operators. Publ. "science", M., 1969.

10. G. I. Makarov, V. V. Novikov. In the collection "Problems of diffraction and propagation of waves", iss. I, page 96, publ. of LGU, 1962.

11. V. I. Smirnov. Course of advanced calculus, Vol. III, part 2. GITTL, M., 1953.

Page 33.

# ELECTROMAGNETIC FIELD IN A PLANE THIN WAVEGUIDE.

G. I. Makarov, V. V. Novikov.

In the present work electromagnetic fields, excited by vertical electric dipole in the three-layered medium with plane interfaces (Fig. 1), will be studied. It is assumed that lower half-space ( $z < 0$ ) possesses infinite conductivity, the properties of layer  $0 \leq z \leq h$  coincide with the properties of vacuum, and upper half-space ( $z > h$ ) represents homogeneous medium with dielectric constant  $\epsilon_m$  and conductivity  $\sigma$ . Value  $\epsilon_m$  can take both positive and negative values. The latter/last case is realized, when upper half-space is formed by cold plasma. In its setting this problem coincides with the problem, examined in the preceding/previous work of the authors [1], where the general/common/total properties of the eigenvalues of transverse operator  $L_z$  were investigated. The problem about the propagation of electromagnetic waves in the flat/plane waveguide was examined by many authors, in particular L. M. Berkhovskikh in monograph [2].



However, in this work the series/row of thin and interesting, from our point of view, effects either is not examined completely or it is examined inaccurately. The fact is the main result of our preceding/previous investigation [1] that the discrete/digital part of the spectrum of operator  $L$  consists in the case  $\epsilon_m > 0$  of a finite number <sup>1</sup> of the eigenvalues, the algebraic multiplicity of each of which can reach two.

FOOTNOTE <sup>1</sup>. Not denumerable, as it was assumed in works [2], [3].

ENDFOOTNOTE.

A number of points of discrete spectrum (each of which is compared with the normal wave) depends on the properties of upper half-space and thickness of waveguide  $h$ . It is calculating only, if  $\epsilon_m < 0$  (this case in the work [2] it was not examined). But if  $\epsilon_m > 0$ , the number of normal waves, which participate in the representation of fields, it is always certainly and the less, the thinner the waveguide. With  $h$  sufficient small ones the discrete/digital part of the spectrum can be in all of one eigenvalue (i.e. in the decomposition it is present only one normal wave) or even be empty.

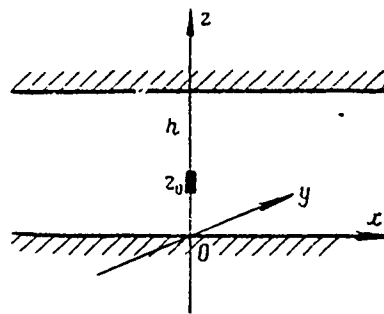


Fig. 1.

Page 34.

However, in the case of the approximate impedance setting <sup>1</sup> the spectrum is purely discrete/digital and without depending on the sizes/dimensions of waveguide and properties of upper half-space consists of a denumerable number of isolated points.

FOOTNOTE <sup>1</sup>. In this setting the dependence of the given surface impedance  $\delta$  on the eigenvalue of transverse operator is ignored.  
ENDFOOTNOTE.

The properties of normal waves for this case are sufficiently well studied with the help of direct variational methods [4]. Thus with small  $h$  the impedance setting proves to be inapplicable, and for this very reason the study of thin waveguides is of special interest.

§ 1. Representation of the solution in the form of the sum of normal, quasi-normal and sky waves.

In order to avoid the appearance of bulky formulas, we will subsequently consider that the source and observation point are arranged/located on the interface with lower half-space ( $z=z_0=0$ ). If we use now formula (1) of work [1] and to switch over from the vector potential  $A$  to the components of electromagnetic field, then it will seem that vertical component of electric field takes the following form: <sup>1</sup>

$$E_z = \frac{iP_0}{4\pi\epsilon_0} \int_{-\infty}^{+\infty} \frac{\lambda^3 H_0^{(1)}(\lambda r)}{\sqrt{k^2 - \lambda^2}} F(\lambda, h) d\lambda, \quad (1.1)$$

where

$$F(\lambda, h) \equiv \frac{\sqrt{k^2 - \lambda^2} \cos \sqrt{k^2 - \lambda^2} h - \frac{i \sqrt{k_2^2 - \lambda^2}}{\epsilon_m} \sin \sqrt{k^2 - \lambda^2} h}{\frac{\sqrt{k_2^2 - \lambda^2}}{\epsilon_m} \cos \sqrt{k^2 - \lambda^2} h - i \sqrt{k^2 - \lambda^2} \sin \sqrt{k^2 - \lambda^2} h}, \quad (1.2)$$

$$k_2 \equiv k \sqrt{\epsilon_m},$$

$k$  - wave number in the vacuum, and  $P_0$  - complete dipole moment of source, connected with current  $I$ , introduced in [1], by the relationship/ratio

$$P_0 = \frac{iIh}{\omega}.$$

FOOTNOTE <sup>2</sup>. We assume that with the sufficiently large  $|\lambda|$  let us assume that the integration occurs in the first quadrant along beam  $\lambda = |\lambda|e^{i\epsilon}$ ,  $\epsilon > 0$ , and secondly  $\lambda = -|\lambda|e^{-i\epsilon}$ . ENDFOOTNOTE.

Fixation of branch  $\sqrt{k^2 - \lambda^2}$  is arbitrary. on plane  $(\lambda)$  from the points  $\pm k$ , the sections/cuts along the lines

$$\operatorname{Im} \sqrt{k^2 - \lambda^2} = 0 \quad (1,3)$$

are carried out and it is assumed that on the upper sheet

$$\operatorname{Im} \sqrt{k^2 - \lambda^2} \geq 0. \quad (1,4)$$

Page 35.

Expansion (1.1) contains both the continuous and discrete/digital of the part of the spectrum. As in [1], we will identify integral (1.1), propagated over both shores of section/cut, with the expansion in terms of the continuous part of the spectrum, and the deductions in zero denominators (1.2), which are isolated with the coincidence of duct/contour (1.1) with the duct/contour, which encompasses section/cut, with the normal waves (or eigenfunction expansion of

transverse operator). The case of multiple poles will correspond so that in expansion there participate also the associated functions <sup>1</sup>.

FOOTNOTE <sup>1</sup>. In work [1] it is shown that with the real  $\omega$  the algebraic multiplicity does not exceed two. ENDFOOTNOTE.

Together with the section/cut, let us lead on both copies of plane  $(\lambda)$  from the point  $\lambda=k_2$ , the half-lines, whose equation (see Fig. 2) has the form:

$$\begin{aligned} \operatorname{Re} \lambda &= \operatorname{Re} k_2, \\ \operatorname{Im} \lambda &\geq \operatorname{Im} k_2. \end{aligned} \quad (1.5)$$

Let us assume that

$$|k_2 r| > 1, \quad (1.6)$$

then on the entire half-line (1.5) it will be possible to use the simplest asymptotic representation of the Hankel function it will seem that the half-lines (1.5) present the duct/contour of the most rapid descent for integral (1.1). Therefore for the determination of asymptotic representations (1.1) according to parameter (1.6) we had to combine the way of integration in (1.1) with the half-lines (1.5). In this case we will cross certain number of poles of expression (1.2) and will be isolated a finite or denumberable number of the terms outside the integral. One should stress that obtained thus

representation of field will no longer be expansion in the form of the sum of normal waves and integral on the continuous part of the spectrum, since into it the part of the deductions in the poles, arranged/located on the lower sheet, will enter also, and they are not the eigenfunctions of transverse operator. Therefore we will call this sum the sum of normal and quasi-normal waves, and the component which contains integral on the duct/contour of descent - by sky wave.

Page 36.

## § 2. Investigation of the poles of function $F(\lambda, h)$ .

In this paragraph we will attempt to visualize the behavior of zero equations

$$\sqrt{k^2 - \lambda_m^2} \operatorname{tg} \sqrt{k^2 - \lambda_m^2} h = -\frac{i}{\epsilon_m} \sqrt{k^2 - \lambda_m^2} \quad (2,1)$$

depending on the height/altitude of waveguide  $h$ . The corresponding investigations on plane ( $\eta$ )

$$\eta_m \equiv \sqrt{k^2 - \lambda_m^2} h \quad (2,2)$$

for  $\epsilon_m > 0$  were made in the preceding/previous work of the authors [1]. In this case as they will interest mainly thin waveguides.

Therefore here it suffices to study only the rough picture of behavior  $\lambda_m$ . More detailed information will be required only for case of  $h \rightarrow 0$  (i.e. exit points in our old terminology).

With  $h \rightarrow 0$  it can be presented two possibilities:

$$1) \left| \sqrt{k^2 - \lambda_m^2} h \right| \not\rightarrow 0, \quad (2,3)$$

$$h \rightarrow 0$$

$$2) \left| \sqrt{k^2 - \lambda_m^2} h \right| \rightarrow 0. \quad (2,4)$$

$$h \rightarrow 0$$

In the first case

$$\sqrt{k^2 - \lambda_m^2} \rightarrow \frac{m\pi}{h} - \frac{1}{h} \operatorname{arctg} \frac{1}{\epsilon_m} \quad (2,5)$$

$$h \rightarrow 0$$

$$m = 0, \pm 1, \pm 2 \dots$$

The location of root  $\lambda_m$  on the upper or lower sheet of riemann surface depends on the sign of the imaginary part of second term in (2.5). Let us introduce the designations

$$\epsilon_m' \equiv \rho e^{i\varphi}, \quad (2,6)$$

$$\operatorname{arctg} \frac{1}{\epsilon_m} \equiv u + iv. \quad (2,7)$$

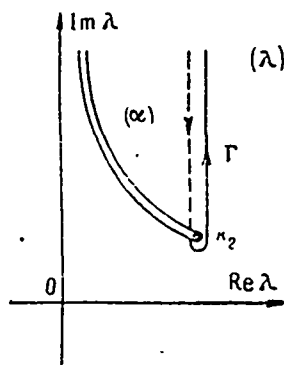


Fig. 2.

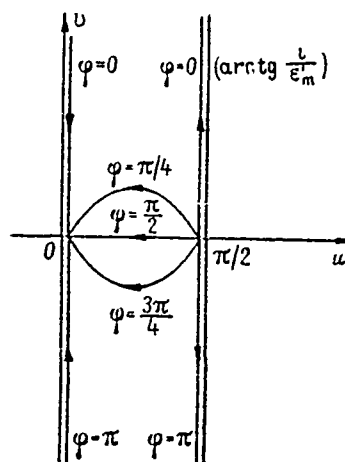


Fig. 3.

Page 37.

If, furthermore, to place for the certainty

$$-\frac{\pi}{2} \leq u \leq \frac{\pi}{2}, \quad (2,8)$$

that by comparatively simple computations it is possible to find the form of the half-lines

$$0 \leq \rho < \infty, \quad \varphi = \text{const} \quad (2,9)$$

on complex plane (2.7). The corresponding lines are represented in Fig. 3, the arrows/pointers indicating the direction of the motion of point on plane (2.7) with the increase/growth  $\rho$ . One should have also in mind that the physically realizable structures correspond to



change  $\varphi$  within the limits

$$0 \leq \varphi \leq \pi. \quad (2,10)$$

It is now not difficult to determine, in what case  $\lambda_m$  with  $h \rightarrow 0$  (exit point is located on the upper sheet of plane  $(\lambda)$ ). For this purpose let us note that if are satisfied the conditions

$$\begin{aligned} \left| m\pi - \operatorname{arctg} \frac{i}{\epsilon_m} \right| &\gg kh, \\ \left| m\pi - \operatorname{arctg} \frac{i}{\epsilon_m} \right| &\gg k \left| \sqrt{\epsilon_m - 1} \right| h, \end{aligned} \quad (2,11)$$

then  $\lambda_m$  it is possible to find from the expression

$$\lambda_m \approx \pm \frac{1}{h} [\pi + i(m\pi - u)]. \quad (2,12)$$

Let us substitute now (2.5) and (2.12) into the left side of transcendental equation (2.1), then it seems that

$$\sqrt{k^2 - \lambda_m^2} \operatorname{tg} \sqrt{k^2 - \lambda_m^2} h \rightarrow - \frac{i}{\epsilon_m} \left[ \frac{m\pi}{h} - \frac{1}{h} \operatorname{arctg} \frac{i}{\epsilon_m} \right]. \quad (2,13)$$

Consequently (2.1) it will be satisfied, if

$$\sqrt{k^2 - \lambda_m^2} \rightarrow \left[ \frac{m\pi}{h} - \frac{1}{h} \operatorname{arctg} \frac{i}{\epsilon_m} \right]. \quad (2,14)$$

From condition (1.4) and formula (2.7) it follows that (2.14) has the place on the upper sheet of plane ( $\lambda$ ) in the case of  $v < 0$ , i.e.

$$\operatorname{Re} \epsilon'_m < 0. \quad (2.15)$$

It is possible also to be convinced of the fact that with  $h \rightarrow \infty$   $\lambda_m$ , those corresponding to the "locked branches" [1], approach point  $\lambda = \pm k$ , and  $\lambda_m$ , corresponding to "infinite branch", to the point

$$\lambda = \frac{k \sqrt{\epsilon'_m}}{\sqrt{\epsilon'_m + 1}}.$$

Page 38.

Since the examination of thick waveguides does not enter into the problem of this work, we will not in detail analyze this case and phenomenon of degeneration, referring to work [1]. Now it is possible to visualize the common picture of behavior  $\lambda_m$  in the dependence on the thickness of waveguide  $h$ . The corresponding trajectories are schematically represented in Fig. 4 and 5. Arrows/pointers showed the direction of the motion of root with increase of  $h$ . Fig. 4 corresponds to medium with  $\epsilon_m > 0$ , while Fig. 5  $\epsilon_m < 0$  (cold plasma). The parts of trajectories  $\lambda_m$ , arranged/located on the lower sheet, are depicted as dotted line.

For the subsequent analysis us it will be necessary to estimate with what  $h$  of trajectory of zeros the half-lines (1.5) intersect. If we use formulas (2.6) (2.7) and (2.12) and to be interested in upper half-plane ( $\lambda$ ), then the height of waveguide  $h_0$ , at which trajectory  $m$  - zero will cross half-line (1.5), it will be located from the condition

$$\beta_0 = \frac{1}{\rho^{3/2}} F(\varphi), \quad \rho > 1,$$

where  $\beta_0 \equiv kh_0$ ,  $F(\varphi) \equiv \frac{|\cos \varphi|}{\cos \frac{\varphi}{2}}$  and  $\beta_0 \approx \frac{1}{\sqrt{\rho}} \frac{|v|}{\cos \frac{\varphi}{2}}$ , if condition  $\rho > 1$  is not satisfied.

Thus, in our approximation/approach, which is determined by force (2.11) with  $\rho > 1$  by the inequalities

$$\begin{aligned} \rho &\gg \left[ \frac{1}{m\pi} F(\varphi) \right]^{2/3} \frac{(\omega)}{\pi \rho_H} \quad m \neq 0, \\ \rho &\gg F^2(\varphi) \frac{(\omega)}{\pi \rho_H} \quad m = 0 \quad (\varepsilon_m < 0), \end{aligned}$$

Key: (1). with.

all  $\lambda_m$  simultaneously cross line (1.5). Exception/elimination is only zero  $\lambda_0$  when  $\varepsilon_m > 0$  (see Fig. 4). It means, if  $\beta < \beta_0$ , then with the coincidence of the duct/contour of integral (1.1) with the duct/contour of most rapid descent (1.5) in the case  $\varepsilon_m > 0$  do not appear deductions at points  $\lambda_m$  of exit point of which they satisfy

condition (2.3). But if  $\varepsilon_m < 0$ , then when  $\beta < \beta_0$ , the solution is present the twice infinite sum of deductions. The waveguide, whose height/altitude satisfies the condition

$$\beta < \beta_0. \quad (2,16)$$

we will subsequently call thin.

$\varphi$ , град.(1)	$F(\varphi)$
0	1
30	0,91
45	0,78
60	0,57
80	0,22
90	0
120	1
135	1,8
150	3,34
170	11,1
180	$\infty$

Key: (1). deg.

Page 39.

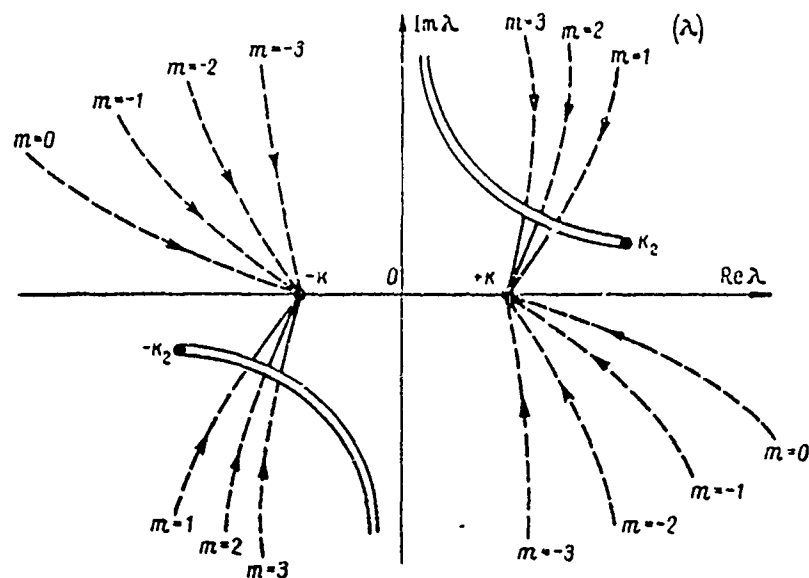


Fig. 4.

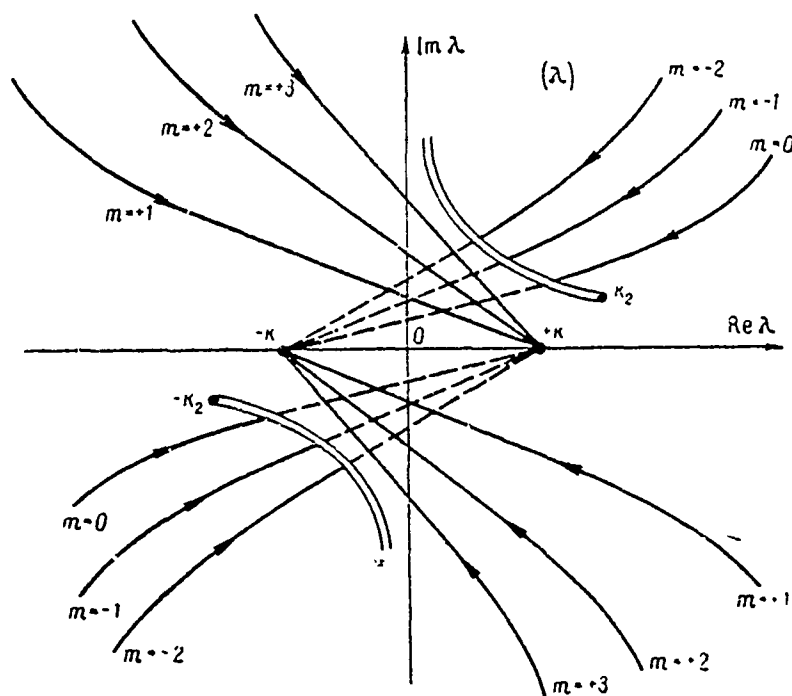


Fig. 5.

Page 40.

In this case, of course, it is assumed that the conditions for applicability (2.11) of formula (2.12) are satisfied also. For convenience in the estimate of the magnitude  $\beta$ , the table gives function  $F(\varphi)$ .

Let us determine order of magnitude  $h_0$  for the waveguide with an infinite-conducting lower wall and with the properties of upper wall, close to the properties of the ionosphere at the low frequencies. Considering that the conductivity of latter  $\sigma_u \approx 10^{-8} \frac{1}{\Omega \cdot m}$ , and  $f \approx 10$  kHz, we will obtain  $h_0 \approx 1.2$  km.

Thus, even in the case of SDV the examined waveguide is in our understanding "thick".

We will be occupied now the study of zero equations (2.1), which satisfies condition (2.4). We will subsequently designate this zero through  $\lambda(^{\circ})$ . Let

$$\lambda^{(0)} \equiv kx_0. \quad (2.17)$$

Taking into account (2.4) equation (2.1) with sufficiently small  $h$  can be recorded in the form

$$(1 - x_0^2) \beta^2 = - \frac{1}{(\epsilon_m')^2} (\epsilon_m' - x_0^2) \quad (2.18)$$

or

$$x_0^2 = \epsilon_m' + (\epsilon_m')^2 \beta^2 (x_0^2 - 1)^2. \quad (2.19)$$

For solution (2.19) let us use the method of successive approximations, after assuming

$$(x_0)_0 = \sqrt{\epsilon_m'},$$

then it will seem that

$$(x_0)_1 = \sqrt{\epsilon_m'} + \frac{\beta^2}{2} F^2(\epsilon_m') \left[ 1 + O(\beta^2) \left| \epsilon_m' (\epsilon_m' - 1) \left( \epsilon_m' + \frac{1}{7} \right) \right| \right], \quad (2.20)$$

$$F(\epsilon_m') \equiv (\epsilon_m')^{3/4} (\epsilon_m' - 1). \quad (2.21)$$

Is not difficult also to find  $(\lambda_0)_1^2$

$$(\lambda^{(0)})_1^2 = k_2^2 + \beta^2 k^2 F_1^2(\epsilon_m'), \quad (2.22)$$

$$F_1(\epsilon_m') \equiv \epsilon_m' (\epsilon_m' - 1). \quad (2.23)$$

Thus, in contrast to exit points  $\lambda_0$  and  $\lambda_m$  exit point  $\lambda^{(0)}$  is



located at finite distance from the origin of coordinates and coincides with branch point. Knowing the argument of function  $F_1(\varepsilon'_m)$ , it is possible to determine, on what sheet is arranged/located the root  $\lambda(^{\circ})$  equation (2.1). Under the condition

$$\frac{\pi}{2} \leq \arg F_1(\varepsilon'_m) < \frac{3}{2} \pi \quad (2.24)$$

the root  $\lambda(^{\circ})$  is arranged/located on the upper sheet. In turn  $\arg F(\varepsilon'_m)$  characterizes position  $\lambda(^{\circ})$  relative to half-line (1.5).

Page 41.

The value of arguments  $F_1(\varepsilon'_m)$  and  $F(\varepsilon'_m)$  they make it possible to judge Fig. 6 and 7. In Fig. 6 they are depicted on plane  $(\varepsilon'_m)$  of line, along which  $\arg F_1(\varepsilon'_m) = \text{const.}$  Numbers by the curves correspond to the numerical value of argument. Fig. 7 makes the same sense, are only here depicted lines  $\arg F(\varepsilon'_m) = \text{const.}$  Ranges of values of  $\varepsilon'_m$ , with which (2.24) it is not made, are designated in Fig. 6 by shading. With such values  $\varepsilon'_m$  the root  $\lambda(^{\circ})$  transcendental equation (2.1) is arranged/located on the lower sheet of plane  $(\lambda)$ . With the combining of the circuit of integration in (1.1) with the duct/contour of the most rapid descent, which proceeds from the point  $\lambda=k$ , (half-line (1.5)), we had to take into account deduction in the pole  $\lambda(^{\circ})$ , if the latter is arranged/located somewhere on the upper sheet, with

exception of region ( $\alpha$ ) (Fig. 2), or on the lower - in region ( $\alpha$ ).  
 Being turned to Fig. 6 and 7 not difficult to establish that if

$$\begin{aligned} \arg F(\varepsilon_m') &> \frac{\pi}{4}, \\ \arg F_1(\varepsilon_m') &\leq \frac{\pi}{2}, \end{aligned} \quad (2,25)$$

then  $\lambda(^{\circ})$  is located on the lower sheet in region ( $\alpha$ ). But if

$$\begin{aligned} \arg F_1(\varepsilon_m') &\geq \frac{\pi}{2}, \\ \arg F(\varepsilon_m') &\leq \frac{5}{4}\pi, \end{aligned} \quad (2,26)$$

then at  $\lambda(^{\circ})$  is arranged/located on the upper sheet out of region ( $\alpha$ ). Of the aforesaid it above follows that with fulfillment (2.25) or (2.26) the strain of duct/contour (1.1) must be accompanied by the addition of deduction in the pole  $\lambda(^{\circ})$ . Uniting (2.25) and (2.26), we will obtain the condition

$$\frac{\pi}{4} \leq \arg F(\varepsilon_m') \leq \frac{5}{4}\pi, \quad (2,27)$$

with fulfillment of which deduction enters into field expression. In Fig. 7 shading isolated ranges of values  $\varepsilon_m'$  in which the deduction in the pole  $\lambda(^{\circ})$  should not be considered.

On this we finish the research of the dynamics of the poles of transcendental equation (2.1). The obtained results make it possible

to pass to the conclusion/output of analytical field expressions in the thin waveguide.

### § 3. Field in the thin waveguide.

We will consider condition (1.6) as that made and let us represent field in the form of the following sum:

$$E_z = E_z^{(1)} + E_z^{(2)}. \quad (3.1)$$

Page 42.

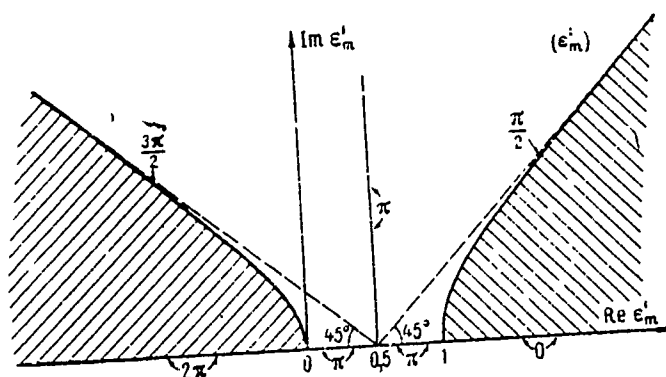


Fig. 6.

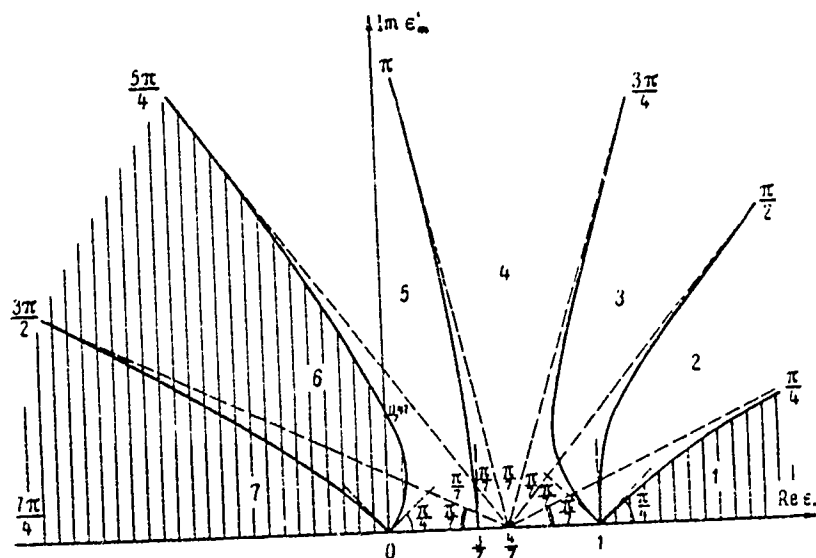


Fig. 7.

Page 43.

To component/term/addend  $E_z^{(1)}$  we will carry integral on the half-line (1.5) and deduction, which corresponds to pole at point  $\lambda(0)$  (if such it is necessary to consider). Then it seems that  $E_z^{(2)}$

are encompassed the deductions in poles  $\lambda_m$ . As it was shown in the preceding/previous paragraph, in the case  $\epsilon_m > 0$  and thin waveguide such deductions must not be considered. Therefore, if  $\epsilon_m > 0$ , then

$$E_z = E_z^{(1)}. \quad (3,2)$$

But if  $\epsilon_m < 0$ , then with the coincidence of initial duct/contour with the duct/contour of descent will be crossed all of pole  $\lambda_m$ . In this case  $E_z^{(2)}$  will be represented in the form of the twice infinite sum of normal waves. Let us consider first component/term/addend  $E_z^{(1)}$ . Taking into account (1.6), let us replace the Hankel function with its asymptotic representation and we deform the duct/contour of the integration. As a result it will prove to be

$$E_z^{(1)} = I + P, \\ I = \frac{e^{\frac{i\pi}{4} P_0}}{4\pi\epsilon_0} \sqrt{\frac{2}{\pi r}} \int \frac{\sqrt{\lambda} \lambda^2}{\sqrt{k^2 - \lambda^2}} F(\lambda, h) e^{i\lambda r} d\lambda, \quad (3,3)$$

where  $F(\lambda, h)$  is determined by formula (1.2) and through  $P$  it is designated deduction in the pole  $\lambda(0)$  (if the latter enters into the solution). The form of circuit  $G$  is represented in Fig. 8.

Let us pass from variable  $\lambda$  to by the variable  $u$  according to the formula

$$\lambda = k_2 + iu^2. \quad (3,4)$$

Then it seems that the coordinate of pole  $\lambda(^{\circ})$  on the plane (u) will be represented in the form

$$u_0 = \sqrt{\frac{k}{2}} \beta F(\varepsilon'_m) e^{-i \frac{\pi}{4}}. \quad (3,5)$$

Point  $u=0$  is saddle point of integrand I. In the vicinity of this point

$$\begin{aligned} \sqrt{k^2 - \lambda^2} &\approx \sqrt{2k_2} u e^{-i \frac{\pi}{4}}, \\ 0 &\leq \arg \sqrt{k_2} \leq \frac{\pi}{4}, \end{aligned} \quad (3,6)$$

$u < 0$  corresponding to upper, and  $u > 0$  - to lower sheet of plane ( $\lambda$ ).

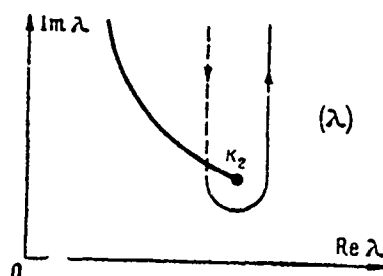


Fig. 8.

Page 44.

Let us assume, furthermore,

$$\sqrt{k^2 - \lambda^2} \approx e^{i \frac{\pi}{2}} k \sqrt{\varepsilon'_m - 1}, \quad (3,7)$$

where the fixation of branch  $\sqrt{\varepsilon'_m - 1}$  is arbitrary. Considering as that made the inequality

$$|\beta \sqrt{\varepsilon'_m - 1}| < 1, \quad (3,8)$$

escaping/ensuing from assumption about the fact that waveguide thin, let us represent  $I$  in the form

$$I = I_1 + I_2, \quad (3,9)$$

where

$$I_1 = \frac{k_2^2 P_0}{2\pi\epsilon_0} \frac{e^{ik_1 r}}{r} \frac{\epsilon_m'}{\sqrt{\pi}} \int_{-\infty}^{+\infty} \frac{v e^{-v^2}}{v + \sqrt{sr}} dv, \quad (3,10)$$

$$I_2 = \frac{k_2^2 P_0}{2\pi\epsilon_0} \frac{e^{ik_1 r - i \frac{3}{r} \pi}}{r} \sqrt{\epsilon_m'} \sqrt{\frac{2}{\pi k r}} \int_{-\infty}^{+\infty} \frac{v^2 e^{-v^2}}{v + \sqrt{sr}} dv, \quad (3,11)$$

$$\sqrt{s} \equiv \frac{e^{i \frac{3}{4} \pi}}{\sqrt{2}} \sqrt{k} \beta F(\epsilon_m'). \quad (3,12)$$

Integrals (3.10) (3.11) are simply connected with the expression for the function of weakening Sommerfield's problem. They are calculated by standard methods [5] and are reduced to the probability integrals of the complex argument. As a result of simple computations we come to the formula

$$I = \frac{k_2^2 P_0}{2\pi\epsilon_0} \epsilon_m' \frac{e^{ik_1 r}}{r} [1 - \beta^2 (\epsilon_m' - 1)] w_1(sr), \quad (3,13)$$

$$w_1(sr) = 1 + 2\sqrt{sr} e^{-sr} \int_{-\infty - i \operatorname{sgn} \operatorname{Im} \sqrt{s}}^{\infty - i \operatorname{sgn} \operatorname{Im} \sqrt{s}} \frac{e^{v^2}}{\sqrt{sr}} dv. \quad (3,14)$$

Second term in the brackets of formula (3.13) appears from integral  $I_2$  (3.11). By virtue of (3.8) this value of the order of an error in

the computations and we it subsequently will not consider.

If we turn now to inequalities (2.25)-(2.27), then it will seem that in the expression for  $E_z^{(1)}$  should be considered the deduction under the condition

$$\operatorname{Im} \sqrt{s} \rightarrow 0, \quad (3.15)$$

P taking the following form:

$$P = - \frac{k_0^2 \rho_0}{2\pi \epsilon_0} \epsilon_m \frac{e^{ik_z r}}{r} [1 - \beta^2 (\epsilon_m - 1)] 2i \sqrt{\pi s r} e^{-sr}. \quad (3.16)$$

Taking into account (3.15) it is possible to represent now sum (3.13) and (3.16) in the following final form:

$$E_z^{(1)} = \frac{k_0^2 \rho_0}{2\pi \epsilon_0} \epsilon_m \frac{e^{ik_z r}}{r} w(sr), \quad (3.17)$$

$$w(sr) = 1 + 2 \sqrt{sr} e^{-sr} \int_{\sqrt{sr}}^{\infty} e^{v^2} dv.$$

Page 45.

We agreed to call value  $E_z^{(1)}$  the sky wave.

In the case  $\epsilon_m > 0$  formula (3.17) characterizes complete field in the thin waveguide. In the form it coincides with the solution of the problem of Sommerfeld about the field of the dipole above the



impedance plane. But if  $\epsilon_m < 0$ , then there should be taken into account still component/term/addend  $E_z^{(2)}$  from (3.1), that characterizes the sum of deductions in poles  $\lambda_m$ , which we call the sum of normal and quasi-normal waves,

$$E_z^{(2)} = \frac{k^3 P_0 e^{i \frac{3}{4} \pi}}{\sqrt{2\pi k r \epsilon_0}} \sum_{m=-\infty}^{m=+\infty} D_m e^{i \lambda_m r}, \quad (3,18)$$

$$D_m = \left(\frac{\lambda_m}{k}\right)^{\frac{3}{2}} \frac{1 - \left(\frac{\lambda_m}{k}\right)^2 - \frac{\lambda_m^2}{k^2 \epsilon_m}}{\sqrt{\epsilon_m - \left(\frac{\lambda_m}{k}\right)^2} + i\beta \left[1 - \left(\frac{\lambda_m}{k}\right)^2 \left(1 + \frac{1}{\epsilon_m}\right)\right] i}, \quad (3,19)$$

moreover it is assumed that  $|kr| > 1$ . Let us note, besides the fact that the waveguide is thin and that with  $h \rightarrow 0$   $|\lambda_m| \rightarrow \infty$ . Then, if they take place of inequality (2.11), expression for  $D_m$  is simplified and it will seem that

$$D_m \approx \frac{1}{i\beta} \left(\frac{\lambda_m}{k}\right)^{\frac{3}{2}}. \quad (3,20)$$

This formula we will use subsequently. However, value  $\lambda_m$  is determined by expression (2.12), in which with  $m > 0$  should be taken the upper, and with  $m = 0$  and  $m < 0$  lower sign.

By such shape of formula (3.17) (3.18) and (3.20) they solve the problem about the determination of field in the flat/plane thin waveguide. The following paragraph will be dedicated to their analysis.

## § 4. Fundamental laws governing the field in the thin waveguide.

The investigation of expression for  $E_z$  let us begin from case  $\epsilon_m > 0$ . Then it seems that

$$E_z = E_z^{(1)} \quad (4,1)$$

it suffices to consider expression (3.17). This expression takes the form, characteristic for the solution of the problem of Sommerfeld about the field of the dipole, arranged/located in the uniform half-space, limited by impedance plane.

Page 46.

For coinciding the field in this problem with the field, described by formula (3.17), one should consider that the properties of half-space, in which is arranged/located the dipole, coincide to the properties of the medium, which limits waveguide on top, and the given surface impedance  $\delta$  of plane in Sommerfeld's problem is equal to

$$\delta = e^{i\frac{\pi}{2}} \beta \frac{F(\epsilon'_m)}{\sqrt{\epsilon_m}}.$$

Only formal difference from Sommerfield's problem lies in the fact that in our case sign  $\text{Re} \delta$  is arbitrary.

Let us recall the fundamental properties of function  $w(sr)$ , which, following the terminology of Sommerfield's problem, we will call the function of weakening, and its argument  $sr$  - numerical distance. We will first consider that

$$|sr| < 1, \quad (4,2)$$

i.e. let us consider the case of small numerical distances. Then

$$w(sr) = 1 + i\sqrt{\pi sr} - 2sr. \quad (4,3)$$

It means, if the property of waveguide it satisfies the condition

$$\text{Im} \sqrt{s} > 0, \quad (4,4)$$

then  $|w(sr)|$  decreases with an increase in the distance. However, with the fulfillment of reverse/inverse inequality

$$\text{Im} \sqrt{s} < 0 \quad (4,5)$$

$|w(sr)|$  increases with increase of  $r$ . However, concerning argument  $w(sr)$ , which we will call supplementary phase  $[\arg w(sr) = \varphi_{\text{zon}}(sr)]$ , the latter it increases with increase of  $r$  under the condition

$$\text{Re} \sqrt{s} > 0 \quad (4,6)$$

and it decreases with the reverse/inverse inequality. Let us note that by virtue of (3.12)

$$\arg \sqrt{s} = \frac{3}{4} \pi + \arg F(\epsilon'_m). \quad (4.7)$$

However, on the value  $\arg F(\epsilon'_m)$  with different ones  $\epsilon'_m$  it is possible to judge with the help of Fig. 7. Being turned to this figure, is not difficult to conclude that in the first quadrant (appropriate  $\epsilon'_m > 0$ ) inequality (4.4) has the place in region (1) and in the part of region (6), and inequality (4.6) in region (4) (5) and also in part (6).

If one considers that the phase rate in waveguide  $c_{\phi \text{ волн}}$  is connected with phase rate  $c_{\phi}$  of plane wave in medium  $z > h$  with the relationship/ratio

$$c_{\phi \text{ волн}} = \frac{c_{\phi}}{1 + \frac{1}{\operatorname{Re} k_2} \frac{d\varphi_{\text{волн}}}{dr}}, \quad (4.8)$$

then it is possible to conclude that in regions (1) (2) (3) with small  $|sr|$   $c_{\phi \text{ волн}} > c_{\phi}$  decreases with the increase/growth,  $r$ , and in regions (4) (5) and (6) (partially, since it is examined the first quadrant)  $c_{\phi \text{ волн}} < c_{\phi}$  and increases with increase of  $r$ .

Page 47.

From formula (3.17) it follows also that if

$$\arg \sqrt{s} = \frac{3}{2}\pi, \quad (4.9)$$

then  $\varphi_{\text{aon}} = 0$  with all,  $r$ , whence follows  $c_{\text{p non}} = c_{\text{p}}$ .

Relationship/ratio (4.9) occurs on the line, which divides regions (3) and (4).

Let us consider now the behavior of field with the large numerical distances

$$|sr| \gg 1. \quad (4.10)$$

In this case it is possible to note  $w(sr)$  by its asymptotic representation

$$w(sr) \sim \begin{cases} - \sum_{n=1}^N \frac{(2n-1)!!}{2^n (sr)^n}; \operatorname{Im} \sqrt{s} > 0, \\ 2i \sqrt{\pi sr} e^{-sr} - \sum_{n=1}^N \frac{(2n-1)!!}{2^n (sr)^n}; \operatorname{Im} \sqrt{s} < 0. \end{cases} \quad (4.11)$$

Holding only one member in expansions (4.11), we will obtain

$$w(sr) \sim \begin{cases} -\frac{1}{2sr}; \operatorname{Im} \sqrt{s} > 0, \\ -\frac{1}{2sr} \Phi(sr); \operatorname{Im} \sqrt{s} < 0, \end{cases} \quad (4,12)$$

$$\Phi(sr) = 1 - 4i \sqrt{\pi} (sr)^{3/2} e^{-sr}. \quad (4,13)$$

Most simply field appears, if the properties of upper half-space are described by certain point from region (1). In this case of  $w(sr)$  it behaves just as in the case of the strongly capacitive plane of the Earth:  $|w(sr)|$  monotonically decreases with increase of  $r$ , and  $\varphi_{\text{дон}}$  approaches the constant, equal to

$$\varphi_{\text{дон}}(sr) \rightarrow \pi - \arg s = -\frac{\pi}{2} - 2 \arg F(\epsilon_m). \quad (4,14)$$

$r \rightarrow \infty$

Behavior of  $|w(sr)|$ ,  $\varphi_{\text{дон}}(sr)$  and  $\epsilon_{\text{ф волн}}$  for the waveguide with the properties in question is represented in Fig. 9-11.

Thus, dependence on the distance of field  $E_z$  in the field  $|sr| \gg 1$  is described by factor

$$\frac{e^{ik_z r}}{r^2}, \quad (4,15)$$

but phase rate with  $r \rightarrow \infty$  approaches the phase rate of plane wave in the unbounded medium with the properties of upper half-space.

Let us now move on to the analysis of field at the large numerical distances in the case, when the properties of upper half-space are described by certain point in regions 2-5 (Fig. 7), moreover is examined only that part of region 5, in which  $\varepsilon_m > 0$ .

Page 48.

In the regions  $\text{Im}\sqrt{s} < 0$  indicated and function  $w(sr)$  has asymptotic representation (4.13). We will be occupied the study of the function  $\Phi(sr)$  from (4.13), which let us rewrite in the form

$$\begin{aligned}\Phi(sr) &= 1 + \rho(r) e^{-i|s|r \sin 2\psi + i3\psi - i\frac{\pi}{2}}, \\ \psi &\equiv \arg \sqrt{s}, \\ \rho(r) &\equiv 4\sqrt{\pi} |sr|^{3/2} e^{-|s|r \cos 2\psi}.\end{aligned}\quad (4.16)$$

Being turned to Fig. 7, let us note that the angle  $2\psi$  is changed in the following limits:

$$2\pi \leq 2\psi \leq \frac{5}{2}\pi \quad \text{область (2)}, \quad (4.17)$$

$$\frac{5}{2}\pi \leq 2\psi \leq 3\pi \quad \text{область (3)}, \quad (4.18)$$

$$3\pi \leq 2\psi \leq \frac{7}{2}\pi \quad \text{область (4)}, \quad (4.19)$$

$$\frac{7}{2}\pi \leq 2\psi \leq 4\pi \quad \text{область (5)}. \quad (4.20)$$

Key: (1). region.

It means that in regions (2) and (5)

$$\begin{aligned} \rho(r) &\rightarrow 0, \\ r &\rightarrow \alpha, \end{aligned} \quad (4,21)$$

and in regions (3) and (4)

$$\begin{aligned} \rho(r) &\rightarrow \infty, \\ r &\rightarrow \infty \end{aligned} \quad (4,22)$$



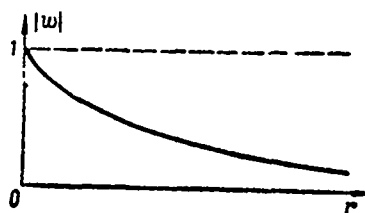


Fig. 9.

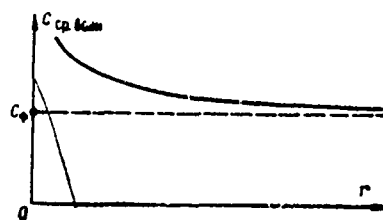


Fig. 10.

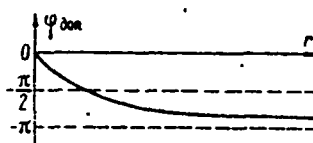


Fig. 11.

Page 49.

Let us consider case (4.21). Function  $\rho(r)$  has a maximum at a distance in this case

$$|s| r_{\max} = \frac{3}{2 \cos 2\psi}, \quad (4.23)$$

moreover

$$\rho(r_{\max}) = \sqrt[3]{2\pi} \left( \frac{3}{2 \cos 2\psi} \right)^{3/2} > 1. \quad (4.24)$$

It is not difficult also to be convinced of the fact that the equation

$$\tilde{\rho}(r^{(i)}) = 1 \quad (4,25)$$

has two roots

$$\begin{aligned} |s| r^{(1)} &\approx \frac{0,11}{\cos 2\psi}, \\ |s| r^{(2)} &\approx \frac{1}{\cos 2\psi} (4 + 3\sin^2 \psi). \end{aligned} \quad (4,26)$$

Form  $\rho(r)$  is represented in Fig. 12.

However, as far as function  $\Phi(sr)$  (4.16) is concerned, in case (4.21) in question on the complex plane ( $\Phi(sr)$ ) depending on  $r$  it will take the form of the spiral, which emerges from point +1. with  $r \rightarrow \infty$  point +1 is limit point. Behavior of  $\Phi$  in region (2) is represented in Fig. 13. In region (5)  $\Phi(sr)$  is analogous spiral, only rotation around point +1 occurs counterclockwise. Let us designate the number of revolutions of spiral around the origin of coordinates through  $m$ . Then limiting value  $\varphi_{\text{don}}$  is located from the formula

$$\begin{aligned} \varphi_{\text{don}} &\rightarrow \pi - \arg s - 2m\pi, \\ r &\rightarrow \infty \end{aligned} \quad (4,27)$$

$$m = 1, 2, 3, \dots$$

In turn Mach number coincides with a number of points of intersection with the spiral of the negative part of the real axis of plane ( $\Phi$ ). However, the latter for region (2) are determined by the following relationships/ratios:

$$\begin{cases} |s| r_k \sin 2\psi - 3\psi + \frac{\pi}{2} = (2k+1)\pi, \\ \rho(r_k) > 1, \end{cases} \quad (4,28)$$
$$k = 0, 1, 2 \dots (m-1).$$

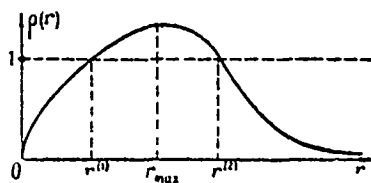


Fig. 12.

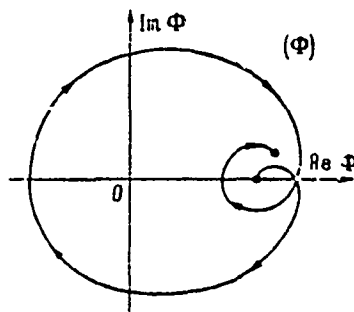


Fig. 13.

Page 50.

Let us attempt to find, with what properties of upper half-space in formula (4.27)  $m=0$ . For this let us note that the smallest root of equation (4.28) corresponds  $k=0$  and is equal to

$$|s|r_0 = \frac{\frac{\pi}{2} + 3\psi}{\sin 2\psi}. \quad (4.29)$$

If it seems that

$$r_0 > r^{(2)}, \quad (4.30)$$

then (4.28) will not have the solutions, i.e., in formula (4.27)  $m=0$ . Considering (4.26) and (4.29), it is possible to give (4.30) the following form:

$$\operatorname{tg} 2\psi \leq \frac{\frac{\pi}{8} + \frac{3}{4}\psi}{1 + \frac{3}{4}\sin^2 \psi}. \quad (4.31)$$

After using the method of the successive approximations (in the zero approximation we assume/set  $\text{tg} 2\psi_0 = \pi/8$ ), it is not difficult to find the values  $\psi$ , which satisfy inequality (4.31),

$$\pi \leq \psi \leq 3,39 \quad (4,32)$$

or

$$\frac{\pi}{4} \leq \arg F(e_m') \leq 1,04. \quad (4,33)$$

The part of region (2), in which is satisfied condition (4.33), we will call "weak" part. Here function  $w(sr)$  has depending on distance comparatively weakly expressed interference character and, in particular,  $|w(sr)|$  it cannot become zero, but limiting value

$\varphi_{\text{don}}(sr)$  is described by formula (4.27) with  $m=0$ . Analogously is isolated "weak" part, also, in region (5), where it is determined by the inequality

$$\frac{5}{4} \pi \geq \arg F(e_m') \geq 3,68. \quad (4,34)$$

Fig. 14 depicts regions (2) and (5) with the chosen "weak" parts. It is now not difficult to visualize the dependence of field in the

waveguide on the distance in the "weak" and "strong" parts of regions (2) and (5).

Let us consider region (2) first. The corresponding graphs for  $|w(sr)|$ ,  $\varphi_{\text{доп}}(r)$  and  $c_{\text{ф волн}}$  are represented in Fig. 15-17.

With the change in the properties of upper half-space, which corresponds to the motion of representative point from the "weak" part of region (2) into the "strong" ( $|s|=\text{const}$ ), the field endures the following changes: a) increases the amplitude of the oscillations of field and their three-dimensional/space period increases; b) establishment  $\varphi_{\text{доп}}(sr)$  occurs at large distances from the source; c) also more slowly is installed  $c_{\text{ф волн}}$  to value  $c_{\text{ф}}$ .

Page 51.

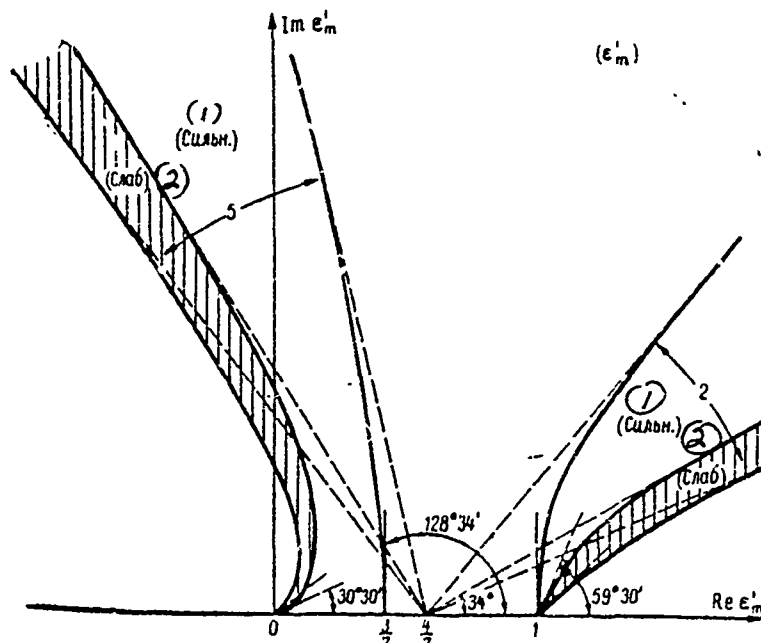


Fig. 14. Key: (1). (Strong). (2). (Weak.).

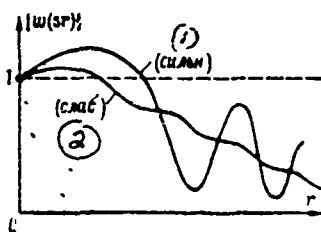


Fig. 15.

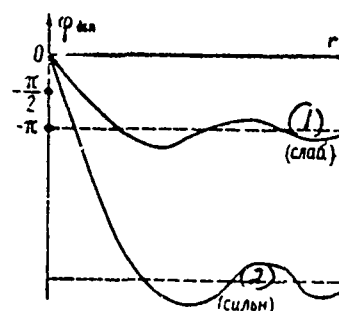


Fig. 16.

Fig. 15 and 16. Key: (1). (Strong). (2). (Weak.).

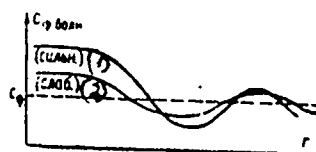


Fig. 17.

Fig. 17. Key: (1). (Strong). (2). (Weak.).

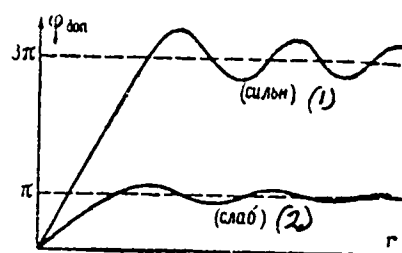


Fig. 18.

Fig. 18. Key: (1). (Strong). (2). (Weak.).

Page 52.

However, with  $r \rightarrow \infty$  field in region (2) and (5) behaves just as in region (1), dependence on the distance as before takes form (4.15).

But if the properties of upper half-space are described by that part of region (5), which corresponds  $\epsilon_m > 0$ , then, as has already been indicated, the properties of fields will be close to case examined above. The character of behavior  $|w(sr)|$  will remain as before, however, concerning  $\varphi_{don}$ , that instead of formula (4.14) should be utilized a relationship/ratio



$$\varphi_{\text{zon}}(sr) \xrightarrow{r \rightarrow \infty} \frac{7}{2}\pi - 2 \arg F(\varepsilon'_m) \quad (4,35)$$

in "weak" part (5) and

$$\varphi_{\text{zon}}(sr) \xrightarrow{r \rightarrow \infty} \frac{7}{2}\pi - 2 \arg F(\varepsilon'_m) + 2m\pi, \quad (4,36)$$

$m = 1, 2, 3 \dots$

in the "strong" part.

FOOTNOTE 1. It is assumed that  $\arg w(0)=0$ . ENDFOOTNOTE.

Dependence  $\varphi_{\text{non}}(sr)$  in the region in question is represented in Fig. 18, and nature of behavior  $\varphi_{\text{non}}(r)$  19. Thus, the values of the phase rate and  $\varphi_{\text{non}}$  in region (5) in contrast to (2) with small  $|sr|$  increase with an increase in the distance from the source.

Let us now move on to the examination of field in the case, when the properties of upper half-space are described by certain point from region (3) or (4) Fig. 7. The behavior of field with small numerical distances was already considered above. We will therefore consider that  $|sr| \gg 1$ . Let us note that in these regions  $\rho(r) \xrightarrow{r \rightarrow \infty} \infty$  and at the large numerical distances from the source in expression (4.13) should be considered only second component/term/addend. Then it seems that (3.17) it will be possible to reduce to the simpler form

$$E_z \approx \frac{k_z^2 P_0}{2\pi\epsilon_0} 2\sqrt{\pi s} \frac{e^{ik_z r - \pi r} e^{-\frac{\pi}{2}}}{\sqrt{r}}. \quad (4.37)$$

If we compare the dependence of field on the distance, described by expression (4.37), with the previously cases (formula (4.15) examined), then it is not difficult to conclude that in regions (3) and (4) occur following properties  $E_z$ .

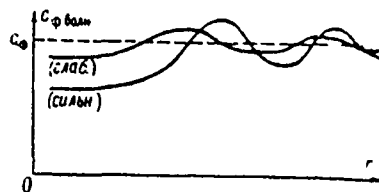


Fig. 19. Key: (1). (Weak.). (2). (Strong).

Page 53.

a) divergence is described by factor  $\frac{1}{\sqrt{r}}$ , which is characteristic for the waveguide problems. However, in the regions (1) (2) and (5) the corresponding factor took the form  $\frac{1}{r^2}$ . This dependence takes usually place in the problem from the field of point source, located near interface in the two-layered (but not three-layered) medium.

b) exponential factor takes now the form

$$e^{ik_1 r - \gamma r} \quad (4,38)$$

This means that the limiting value of phase rates now no longer coincides with the phase rate of plane wave in upper half-space  $C_\phi$  (which is also characteristic for Sommerfield's problem), and it is

determined by the expression

$$(c_{\text{ph no.m}})_{\text{upper}} = \frac{c_{\text{ph}}}{1 - \frac{|s| \sin 2\psi}{\operatorname{Re} k_2}}.$$

It means, in region (3)  $c_{\text{ph no.m}} > c_{\text{ph}}$ , and in region (4)  $c_{\text{ph no.m}} < c_{\text{ph}}$ . The behavior of the phase rates in the dependence on the distance is represented in Fig. 20 (region (3)) and 21 (region (4)). Furthermore, if in all previously cases in question the exponential character of the decrease of field with the distance coincided with the decrease of the plane wave, which is propagated in the medium with the properties of upper half-space, then in this situation the corresponding factor takes the form

$$e^{-[\operatorname{Im} k_1 - |s| |\cos 2\psi|] r}. \quad (4.38a)$$

This means that the field in the waveguide decreases, generally speaking, it is slower than field in the upper half-space. This difference most strongly is expressed on the line, which divides regions (3) and (4). Thus, it proves to be that in the case of media with properties (3) or (4) is observed more clearly the expressed channeling of field. This is connected with the less effective penetration of the latter into the upper half-space.

Let us now move on to the examination of the case, when upper

half-space represents conducting medium with the negative dielectric constant. As has already been indicated, cold plasma possesses such properties.

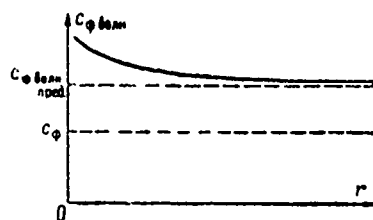


Fig. 20.

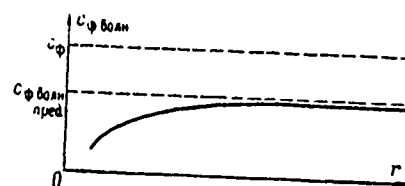


Fig. 21.

Page 54.

For describing the field in the waveguides with similar properties it is necessary in expression  $E_z$  (3.1) to consider also component  $E_z^{(2)}$  of (3.18)-(3.20). If we use formula (2.12), then  $E_z^{(2)}$  will be represented in the form

$$E_z^{(2)} \approx -\frac{k^2 \rho_0}{2\pi \epsilon_0} e^{i\frac{\pi}{4}} \frac{e^{i|v|\frac{r}{h}}}{r} e^{-u\frac{r}{R}} w_2(r), \quad (4.39)$$

$$w_2(r) = \sqrt{\frac{2\pi r}{h}} \frac{1}{\beta^2} \left\{ [|v| + iu]^{3/2} + \sum_{m=1}^{\infty} [i(m\pi - u) + |v|]^{3/2} \times \right. \\ \left. \times e^{- (m\pi - 2u) \frac{r}{h}} \right\}, \quad (4.40)$$

where  $u$  and  $v$  are assigned by formula (2.7), moreover by virtue of (2.8)  $u \leq \pi/2$ . As it follows from formulas (4.39), all waves entering expression  $E_z^{(2)}$ , move with identical phase rate  $c_{\phi}^{(2)} \text{ волн}$ , equal to

$$C_{\text{up}}^{(2)} = \frac{c}{v}, \quad (4.41)$$

where  $c$  - speed of light in the vacuum. The effective depth of penetration of such waves into waveguide  $d_c^{(2)}$  can be found from the formula

$$d_c^{(2)} = \frac{h}{u}. \quad (4.42)$$

If  $|\varepsilon_m| \sim O(0)$ , then, as is evident, for example, from Fig. 3  $u \sim \pi/2$  and  $d_c \sim h$ . As we will see subsequently, in this case component/term/addend  $E_z^{(2)}$  very little in comparison with  $E_z^{(1)}$ . But if  $|\varepsilon_m| \gg 1$ , then

$$\text{arctg} \frac{i}{\varepsilon_m} \approx \frac{l}{\varepsilon_m}$$

it proves to be that

$$\begin{aligned} u &\approx \frac{\frac{a}{\omega \varepsilon_0}}{|\varepsilon_m|^2} \ll 1, \\ v &\approx \frac{|\varepsilon_m|}{|\varepsilon_m|^2} \ll 1, \end{aligned} \quad (4.43)$$

i.e. the depth of penetration  $d_c^{(2)}$  can considerably exceed the thickness of waveguide  $h$ .

Let us now move on to the computation of component/term/addend  $E_z^{(1)}$  from (3.1). Let us preliminarily note that value  $\psi$  from (4.16) in the appropriate regions of the second quadrant of plane  $\varepsilon_m$  is determined by inequalities<sup>1</sup>

$$\begin{aligned} -\frac{\pi}{4} &\leq \psi \leq 0 \text{ область (5),} \\ 0 &\leq \psi \leq \frac{\pi}{4} \text{ область (6),} \\ \frac{\pi}{4} &\leq \psi \leq \frac{\pi}{2} \text{ область (7).} \end{aligned} \quad (4.44)$$

Key: (1). region.

FOOTNOTE <sup>1</sup>. Here from both parts of the inequality unessential for us value  $2\pi$  is subtracted. ENDFOOTNOTE.

Page 55.

It means, for determination  $E_z^{(1)}$  in the part of region (5), which lies in the second quadrant, should be used formula (4.37), and in regions (6) and (7) - by formula (3.17). Let us note, besides the fact that under the conditions

$$\begin{aligned} |\varepsilon_m| &\sim O(0), \\ \operatorname{Re} \varepsilon_m &< 0 \end{aligned} \quad (4.45)$$



makes sense to examine only regions (6) and (7). However, in the latter dependence  $E_z'$  on the distance with the large  $|sr|$  is determined by factor (4.15)

$$\frac{e^{ik_3 r}}{r}.$$

Consequently, for the part of the field, described by component/term/addend  $E_z^{(1)}$ , effective depth of penetration is equal to

$$d_c^{(1)} \sim \frac{1}{k \operatorname{Im} \sqrt{\varepsilon_m}} \quad (4.46)$$

and in the case of small ones in question  $|\varepsilon_m'|$  considerably exceeds  $d_c^{(2)}$ . Thus, case (4.45) is reduced to study  $E_z^{(1)}$  in regions (6) and (7). Taking into account (4.44), it is not difficult to conclude that here  $\operatorname{Im} \sqrt{s} > 0$ , and this means that the field behaves qualitatively just as in region (1). Difference consists only of the fact that here in view of  $\operatorname{Re} \sqrt{s} > 0$   $C_{\phi \text{ with } r \rightarrow \infty} \rightarrow C$  from the side of smaller (but not high) values. The oscillations of phase rate also are not observed.

Let us now move on to the examination of the more interesting case

$$\begin{aligned} |\varepsilon'_m| &\gg 1, \\ \operatorname{Re} \varepsilon_m &< 0, \end{aligned} \quad (4.47)$$

when<sup>1</sup> can prove to be that

$$d_c^{(2)} \sim d_c^{(1)} \quad (4.48)$$

or

$$d_c^{(2)} \gg d_c^{(1)}. \quad (4.49)$$

FOOTNOTE <sup>1</sup>. In the "asymptotic" thin waveguides  $h \rightarrow 0$ ,  $d_c^2 \rightarrow 0$  and cannot be thus. ENDFOOTNOTE.

Page 56.

If it seems that inequality (4.49) occurs, then at the distances from source  $r > d_c^{(1)} E_z \approx \dot{E}_z^{(2)}$ . However, value  $E_z^{(2)}$  is defined as the sum of waves with the cylindrical divergence, i.e., by "waveguide" type waves. Thus, in contrast to previously case (4.45) examined here is observed the more clearly expressed channeling of energy. This channeling was observed when  $\varepsilon_m > 0$  only in regions (3) or (4). In the case (4.46) components/terms/addends  $E_z^{(1)}$  and  $E_z^{(2)}$  are equally essential. Since phase wave velocity, which correspond to these

components/terms/addends, are different, complete field will carry complicated interference character. Especially complicated form will have a field in region (5), where as a result of the presence of deduction P (3.16) interaction of three waves with different phase rates will be observed. However, if together with (4.48) is satisfied condition  $\dot{a}_e^{(2)} \leq a_e^{(1)}$ , then sufficiently far from the source interference will not be observed, since component/term/addend  $E_z^{(2)}$  has, as has already been indicated, cylindrical divergence, but divergence  $E_z^{(1)}$  is determined by factor  $1/r_1$ . Thus, in this case at large distances from the source the "waveguide" character of propagation as before occurs.

#### Literature.

1. G. I. Makarov, V. V. Novikov. This collection, Page 3.
2. L. M. Brekhovskikh. Waves in the laminar media. Publ. of the AS USSR, M., 1957.
3. Ya. L. Alpert. On the propagation of the electromagnetic waves of low frequency above the earth's surface publ. of the AS USSR, M., 1955.
4. G. I. Makarov, V. V. Novikov. In the collection "Problem of

diffraction and propagation of waves", Iss. VII, page 19-33, Publ. of LGU, 1968.

5. V. A. Fok. Radio wave diffraction around the earth's surface. Publ. of the AS USSR M., 1946.

Page 201.

SUPPLEMENT AND REVISION TO THE ARTICLE "On THE TROPOSPHERIC REFRACTION OF RADIO WAVES" [1].

G. I. Makarov, N. P. Tikhomirov.

In work [1] the problem of diffraction radiowave propagation around the Earth upon consideration of the atmosphere heterogeneous in the height/altitude was examined and the approximate analytical expressions for the zero eigenvalue  $t_0$  were obtained.

Page 202.

In particular, with the sufficiently small surface impedance of formula for  $t$ , they take the following form <sup>1</sup>:

with the linear profile/airfoil of the atmospheric heterogeneity

$$t_0 - t_0^0 \approx \frac{q^2}{t_0^0} + \frac{\eta_s}{2t_0^0} - \frac{3}{4}\eta_s^2, \quad (1)$$

with the exponential profile/airfoil at the high ( $\mu \ll 1$ ) frequencies

$$t_0 - t_0^0 \approx \frac{q^2}{t_0^0} + \frac{\eta_s}{2t_0^0} + \frac{\alpha}{1+\alpha} \cdot \frac{\eta_s}{2H} \frac{\frac{4}{3.5}(t_0^0)^3 - \frac{1}{10}}{t_0^0} \mu_s, \quad (2)$$

with the exponential profile/airfoil at the low ( $\mu \geq 1$ ) frequencies

$$t_0 - t_0^0 \approx \frac{q}{t_0^0} + \frac{\eta_s}{2t_0^0} + \frac{2\alpha\alpha_s}{2+\mu^2} \left(1 + \frac{\mu^2}{2t_0^0}\right). \quad (3)$$

FOOTNOTE <sup>1</sup>. Here we do not dwell on the designations, they completely coincide to designations in [1]. ENDFOOTNOTE.

First term in the right side in (1) corresponds to the concept

of an equivalent radius, second term appears due to the modified impedance, and the third - due to Schwarz's derivative in the equation for the eigenfunctions of problem. First two terms in (2) make the same sense, that also in formula (1), third composed here appears as a result of a difference in the exponential profile/airfoil from the linear. In formula (3) first term corresponds to homogeneous atmosphere, the second is caused by the effect of atmospheric heterogeneity on surface impedance, and the third considers tropospheric refraction. For the evaluation of the role of each component/term/addend in (1) (2) in [1] phase rate and attenuation of zero normal wave were calculated; however, during the computations was allowed the error, as a result of which the numbers given in Table 1.2 in [1] do not correspond to formulas (1) (2), i.e., to formulas (49) (55) on numbering [1].

Table 1.

f, kHz (1)	$\nu_s$	$\nu_{\text{ph},s}^{(0)}$ , S			$\alpha_s^{(0)}$ , K	
		a	b	u	a	b
0,5	0,029	0,980546	0,980275	0,980299	$3,436 \cdot 10^{-2}$	$3,438 \cdot 10^{-2}$
5,0	0,0063	0,995744	0,995731	0,995731	$7,304 \cdot 10^{-3}$	$7,381 \cdot 10^{-3}$
10,0	0,0040	0,997314	0,997309	0,997309	$4,664 \cdot 10^{-3}$	$4,655 \cdot 10^{-3}$
50,0	0,0014	0,999080	0,999079	0,999079	$1,595 \cdot 10^{-3}$	$1,594 \cdot 10^{-3}$

Note: a) without taking into account second and third terms in (1),  
 b) taking into account of second term, c) taking into account second  
 and third terms. The constant c during the computations was  
 assumed/set equally  $3 \cdot 10^8$  to m/s.

Key: (1). kHz.

Page 203.

Table 1, 2 with the corrected values of rate and attenuation of zero  
 normal wave when  $\delta_s = 0$ . are given below. Furthermore, for the  
 evaluation of the role of third component/term/addend in (3) here is  
 given Table 3, in which for the series/row of frequencies are given  
 phase rate and attenuation of zero mode. Table 1 corresponds to  
 linear profile/airfoil, moreover in contrast to [1], into it are  
 introduced also the values of the phase rate upon consideration of  
 Schwarz's derivative.

From Table 1 it is evident that with the linear profile/airfoil, which corresponds to the lower layers of the earth's atmosphere, at frequencies of higher than 5 kHz the effect of the modified impedance on the phase rate affects only in the fifth significant place, and attenuation - in the third. The effect of Schwarz's derivative on these frequencies is generally is negligibly small.

A difference in the exponential profile/airfoil from the linear at frequencies of higher than 10 MHz, as can be seen from Table 2, virtually does not affect the phase rate of zero normal wave, but in the attenuation it is developed only in the third significant place. In Table 2 case b, which corresponds to the account of second term in (2) is not reflected; its contribution to the eigenvalue at the frequencies in question can be disregarded/neglected. The role of tropospheric refraction at the low ( $\mu \geq 1$ ) frequencies is visible of given below Table 3.

The effect of the modified apparent resistance on the phase rate and the attenuation of zero mode at frequencies is above 10 kHz, as are shown calculations, the second order of smallness in comparison with the effect of tropospheric refraction; therefore in table 3 case b, which corresponds to the account of second term in (3) is not reflected.



Table 2.

$f, \text{MHz}$ (1)	$\mu$	$v_{\text{par}}^{(0)}/s$		$a^{(0)}/\kappa$	
		a	b	a	b
10.0	0.063	0.999973	0.999973	$4.664 \cdot 10^{-5}$	$4.704 \cdot 10^{-5}$
20.0	0.039	0.999983	0.999983	$2.938 \cdot 10^{-5}$	$2.954 \cdot 10^{-5}$
50.0	0.021	0.999991	0.999991	$1.595 \cdot 10^{-5}$	$1.600 \cdot 10^{-5}$

Note: a) for linear profile/airfoil, c) for the exponential.

Key: (1). MHz.

Table 3.

$f, \text{kHz}$ (1)	$\mu$	$v_{\text{par}}^{(0)}/s$		$a^{(0)}/\kappa$	
		a	b	a	b
10.0	5.63	0.996676	0.996640	$5.776 \cdot 10^{-3}$	$5.718 \cdot 10^{-3}$
30.0	2.71	0.998399	0.998316	$2.777 \cdot 10^{-3}$	$2.683 \cdot 10^{-3}$
50.0	1.93	0.998861	0.998727	$1.975 \cdot 10^{-3}$	$1.864 \cdot 10^{-3}$
100.0	1.21	0.999282	0.999053	$1.244 \cdot 10^{-3}$	$1.138 \cdot 10^{-3}$

Note: a) for homogeneous medium, c) taking into account third component/term/addend in (3).

Key: (1). kHz.

Page 204.

In conclusion the authors express appreciation to L. N. Lutchenko,

that indicated the nonconformity of those given in [1] Table 1, 2 to Formulas (49) (55).

#### Literature.

1. G. I. Makarov, N. P. Tikhomirov. In the collection "Problem of diffraction and propagation of waves", Iss. X, Publ. of LGU 1970.